A computational study of the $HO_2 + SO_3 \rightarrow HOSO_2 + {}^3O_2$ reaction catalyzed by water monomer, water dimer and small clusters of sulfuric acid: kinetics and atmospheric implications

Yongqi Zhang [a,#], Yang Cheng [a,#], Tianlei Zhang [a,*], Rui Wang [a], Jianwei Ji [a], Yu Xia[b], Makroni Lily [c,*], Zhuqing Wang [d,*], Balaganesh Muthiah [e]

[a] *Institute of Theoretical and Computational Chemistry, Shaanxi Key Laboratory of Catalysis, School of Chemical & Environment Science, Shaanxi University of Technology, Hanzhong, Shaanxi 723001, P. R. China*

[b] *School of Mechatronics Engineering, Guizhou Minzu University, Guiyang, Guizhou 550025, P. R. China*

[c] *Environmental Research Institute, Shandong University, Qingdao, Shandong 266237, P. R. China*

[d] *Shandong Key Laboratory of Biophysics, Institute of Biophysics, Dezhou University, Dezhou, Shandong 253023, P. R. China*

[e] *Department of Chemistry, National Taiwan University, Taipei 106, Taiwan*

S. NO	Caption
S1	**Fig. S1** The optimized geometries for the species involved in the $HO_2 + SO_3$ reaction at several different levels of theory
S2	**Table S1** The energy barriers (Δ*E*) and unsigned error (UE) (kcal·mol^{-1}) for the $HO_2 + SO_3 \rightarrow HOSO_2 + {}^3O_2$ reaction at different theoretical methods with zero-point energy (ZPE) correction
S3	**Fig. S2** Optimized geometries and binding energies of the reactant complexes $HO_2\cdots X$ (X = H_2O, $(H_2O)_2$, H_2SO_4, $H_2SO_4\cdots H_2O$ and $(H_2SO_4)_2$) and $SO_3\cdots X$ at the CCSD(T)/aug-cc-pVTZ//M06-2X/6-311+G(2*df*,2*pd*) level of theory
S4	**Fig. S3** The optimized geometries and electric energies (in Hartree-Fock) of $HO_2\cdots SO_3\cdots H_2SO_4$ at the M06-2X/6-311+G(2*df*,2*pd*) level of theory
S5	**Fig. S4** The optimized geometries and electric energies (in Hartree-Fock) of $HO_2\cdots SO_3\cdots H_2SO_4\cdots H_2O$ at the M06-2X/6-311+G(2*df*,2*pd*) level of theory
S6	**Fig. S5** The optimized geometries and electric energies (in Hartree-Fock) of $HO_2\cdots SO_3\cdots (H_2SO_4)_2$ at the M06-2X/6-311+G(2*df*,2*pd*) level of theory
S7	**Fig. S6** The results of IRC calculations for all the transition states involved in the $HO_2 + SO_3$ reactions without and with catalyst X (X = H_2O, $(H_2O)_2$, H_2SO_4, $H_2SO_4\cdots H_2O$ and $(H_2SO_4)_2$)
S8	**Fig. S7** Potential energy surface for the unfavorable routes in the $HO_2 + SO_3$ reaction with H_2O at the CCSD(T)/aug-cc-pVTZ//M06-2X/6-311+G(2*df*,2*pd*) level of theory
S9-S10	**Table S2** The equilibrium constant (K_{eq}, in cm^3·molecules^{-1})[a], and concentrations (molecules·cm^{-3}) of complexes $HO_2\cdots H_2O$, $SO_3\cdots H_2O$, $H_2O\cdots HO_2$, $HO_2\cdots (H_2O)_2$, $SO_3\cdots (H_2O)_2$, *c*-$HO_2\cdots H_2SO_4$, *c*-$SO_3\cdots H_2SO_4$, *t*-$HO_2\cdots H_2SO_4$, *t*-$SO_3\cdots H_2SO_4$, *c*-$H_2SO_4\cdots H_2O$, *c*-$HO_2\cdots H_2SO_4\cdots H_2O$, *c*-$SO_3\cdots H_2SO_4\cdots H_2O$, *t*-$H_2SO_4\cdots H_2O$, *t*-

* Corresponding authors. Tel: +86-0916-2641083, Fax: +86-0916-2641083.

e-mail: ztianlei88@l63.com (T. L. Zhang); lilymakroni@outlook.com (M. Lily); wangzq128@163.com (Z. Q. Wang).

# Yongqi Zhang and Yang Cheng have contributed equally to this work.

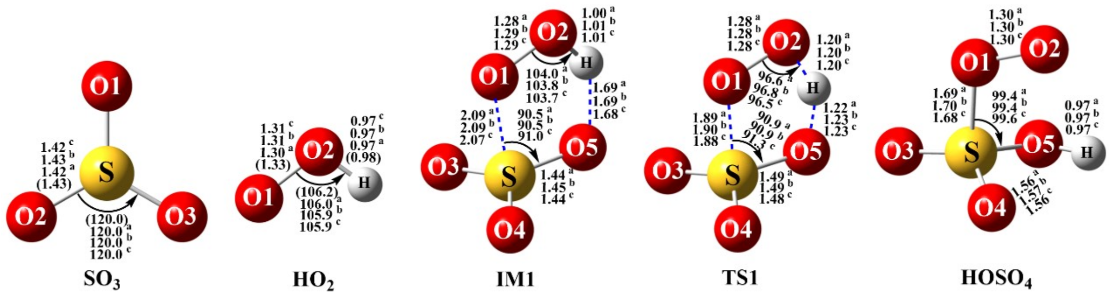

Fig. S1 The optimized geometries for the species involved in the HO_2 + SO_3 reaction at several different levels of theory

[a, b, c and d] respectively represent the values obtained at the M06-2X/6-311+G(2*df*,2*pd*), M06-2X/aug-cc-pVTZ, M06-2X/aug-cc-pV(T+d)Z and M06-2X/6-311++G(2*df*,2*pd*) level of theory. (The values in parentheses were the experimental values; bond length is in angstrom and angle is in degree.)

In order to check whether the geometric parameters of the reactants, pre-reactive complexes, transition states and products for the HO_2 + SO_3 reaction can give good and reliable results at the M06-2X/6-311+G(2*df*,2*pd*) level, we have re-optimized all equilibrium structures at the M06-2X/aug-cc-pVTZ and M06-2X/aug-cc-pV(T+d)Z levels. As shown in Fig. S1, for the calculated geometrical parameters of the above species, the mean absolute deviation of calculated bond distances and bond angles between the M06-2X/6-311+G(2*df*,2*pd*) level and the M06-2X/aug-cc-pVTZ level were 0.005 Å and 0.1°, respectively. Meanwhile, when comparing the M06-2X/6-311+G(2*df*,2*pd*) and M06-2X/aug-cc-pV(T+d)Z levels, it was found that the calculated the mean absolute deviation of calculated bond distances and bond angles were found to be 0.006 Å and 0.23°. Therefore, the bond lengths and angles for the reactants, pre-reactive complexes, transition states and products at the M06-2X/6-311+G(2*df*,2*pd*) level are close to those from the M06-2X/aug-cc-pVTZ and M06-2X/aug-cc-pV(T+d)Z method. In addition, the calculated bond distances and bond angles for the M06-2X/6-311+G(2*df*,2*pd*) level agree well with the corresponding experimental values (From the NIST chemistry webbook, http://webbook.nist.gov/chemistry.). Therefore, due to its efficiency, the M06-2X/6-311+G(2*df*,2*pd*) was adopted to optimize the geometries of all stationary points for the HO_2 + SO_3 reactions.

Table S1 The energy barriers (ΔE) and unsigned error (UE) (kcal·mol^{-1}) for the HO_2 + SO_3 → $HOSO_2$ + $^3O_2$ reaction at different theoretical methods with zero-point energy (ZPE) correction

Methods	ΔE ^{a}	ΔE^b	ΔE^c	UE
W3X-L//M06-2X/6-311+G(2*df*,2*pd*)	-10.6	-9.7	-14.4	0.00
W2X//M06-2X/6-311+G(2*df*,2*pd*)	-10.7	-10.0	-14.8	0.38
CCSD(T)/aug-cc-pVTZ//M06-2X/6-311+G(2*df*,2*pd*)	-10.5(-10.48)^d	-9.8(-9.68)^d	-14.2(-13.81)^d	0.13
CCSD(T)/aug-cc-pVTZ//M06-2X/6-311++G(2*df*,2*pd*)	-10.5(-10.48)^d	-9.8(-9.68)^d	-14.2(-13.81)^d	0.13
CCSD(T)/aug-cc-pVTZ//M06-2X//aug-cc-pVTZ	-10.4	-9.8	-14.1	0.20
CCSD(T)/aug-cc-pV(T+d)Z//M06-2X//aug-cc-pV(T+d)Z	10.8	10.1	14.8	0.33
DLPNO-CCSD(T)-F12/cc-pVDZ-F12//M06-2X/6-311+G(2*df*,2*pd*)	-10.6	-9.9	-14.8	0.20
CCSD(T)-F12a/cc-pVDZ-F12//M06-2X/6-311+G(2*df*,2*pd*)	-11.7	-11.0	-15.8	1.27
CCSD(T)/cc-pVTZ//M06-2X/6-311+G(2*df*,2*pd*)	-9.4(-9.44)^d	-8.9(-8.67)^d	-12.4(-12.64)^d	1.33
CCSD(T)/aug-cc-pVDZ//M06-2X/6-311+G(2*df*,2*pd*)	-9.1	-7.3	-11.7	2.17
CCSD(T)/cc-pVDZ//M06-2X/6-311+G(2*df*,2*pd*)	-7.5	-5.4	-7.1	4.9

$^{a,\ b\ \text{and}\ c}$ respectively denote the species of pre-reactive complexes, transition states and post-reactive complexes involved in HO_2 + SO_3 reaction.
^{d} The value taken from reference 1.

To further confirm the reliability of the M06-2X/6-311+G(2*df*,2*pd*) method, the CCSD(T)/aug-cc-pVTZ single point energies based on the M06-2X/6-311+G(2*df*,2*pd*) optimized geometries were redefined. As presented in Table S1, the relative energy of pre-reactive complexes, transition states and products to the reactants at the CCSD(T)/aug-cc-pVTZ//M06-2X/6-311+G(2*df*,2*pd*) level was respectively -10.5 kcal·mol^{-1}, -9.8 kcal·mol^{-1} and -14.2 kcal·mol^{-1}, which were consistent with the corresponding predicted values at the CCSD(T)/aug-cc-pVTZ//M06-2X//aug-cc-pVTZ level. Similarly, the energies difference at the CCSD(T)/aug-cc-pVTZ//M06-2X//aug-cc-pVTZ, CCSD(T)/aug-cc-pVTZ//M06-2X/6-311+G(2*df*,2*pd*) and CCSD(T)/aug-cc-pV(T+d)Z//M06-2X// aug-cc-pV(T+d)Z levels compared to the relative energies calculated at the W3X-L//M06-2X/6-311+G(2*df*,2*pd*) level, were less than 0.33 kcal·mol^{-1}. This suggests that the relative energies obtained at the CCSD(T)/aug-cc-pVTZ//M06-2X/6-311+G(2*df*,2*pd*) level are also reasonable. Considering the computational accuracy and cost, the CCSD(T)/aug-cc-pVTZ//M06-2X/6-311+G(2*df*,2*pd*) method was chosen to calculate the single point energies of all species for the HO_2 + SO_3 reactions.

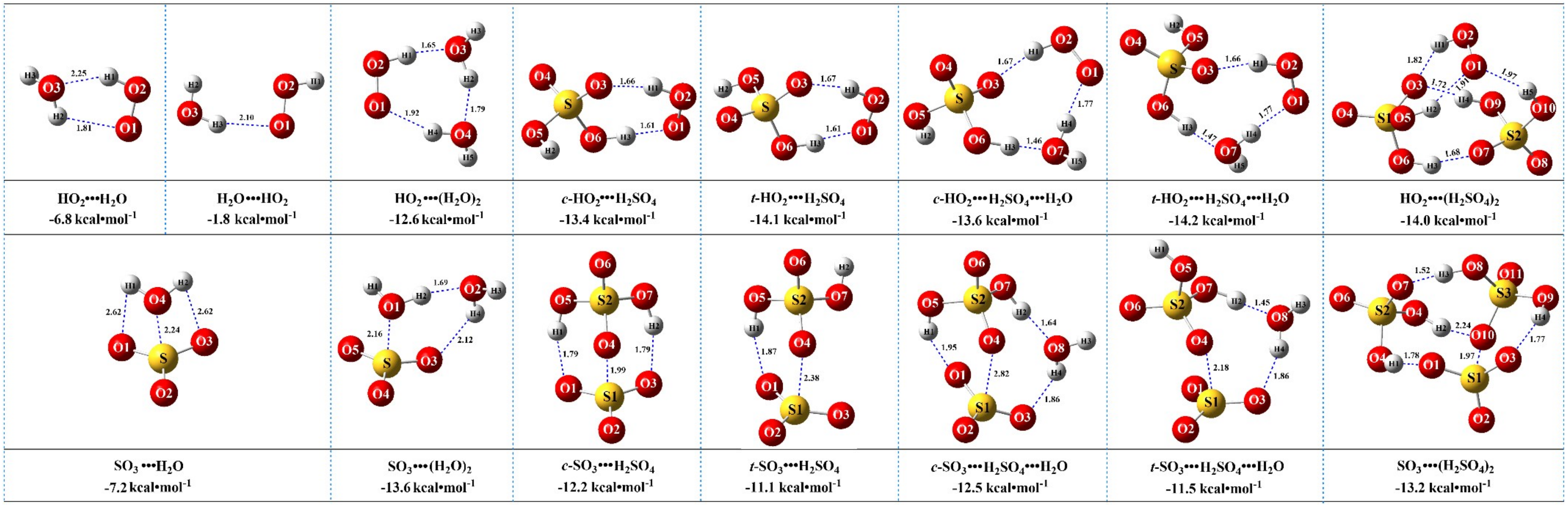

Fig. S2 Optimized geometries and binding energies of the reactant complexes $HO_2\cdots X$ (X = H_2O, $(H_2O)_2$, H_2SO_4, $H_2SO_4\cdots H_2O$ and $(H_2SO_4)_2$) and $SO_3\cdots X$ at the CCSD(T)/aug-cc-pVTZ//M06-2X/6-311+G(2*df*,2*pd*) level of theory (bond distance in Angstroms and angles in degrees)

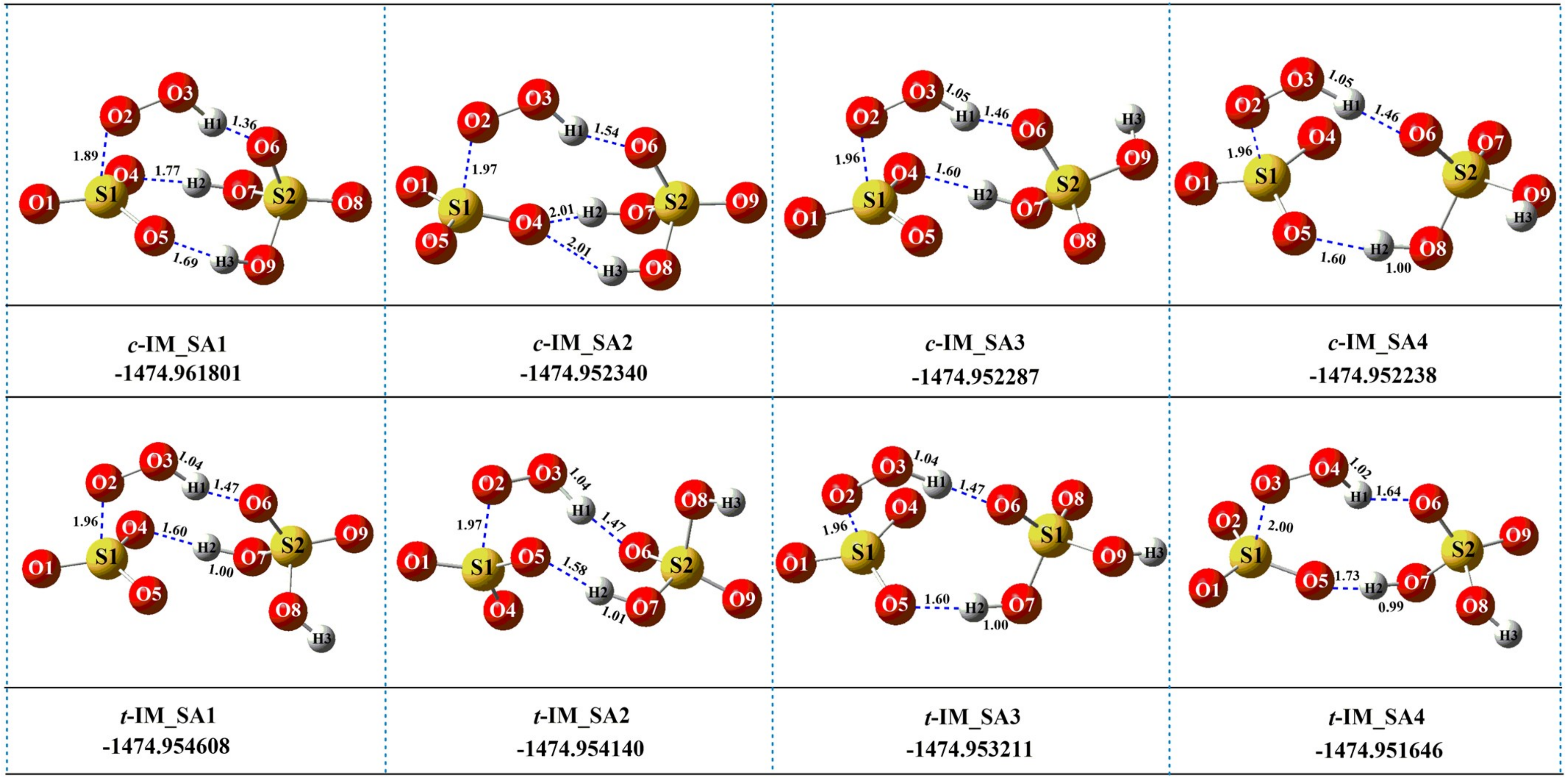

Fig. S3 The optimized geometries and electric energies (in Hartree-Fock) of $HO_2\cdots SO_3\cdots H_2SO_4$ at the M06-2X/6-311+G(2*df*,2*pd*) level of theory (Bond distances in Angstroms and angles in degrees)

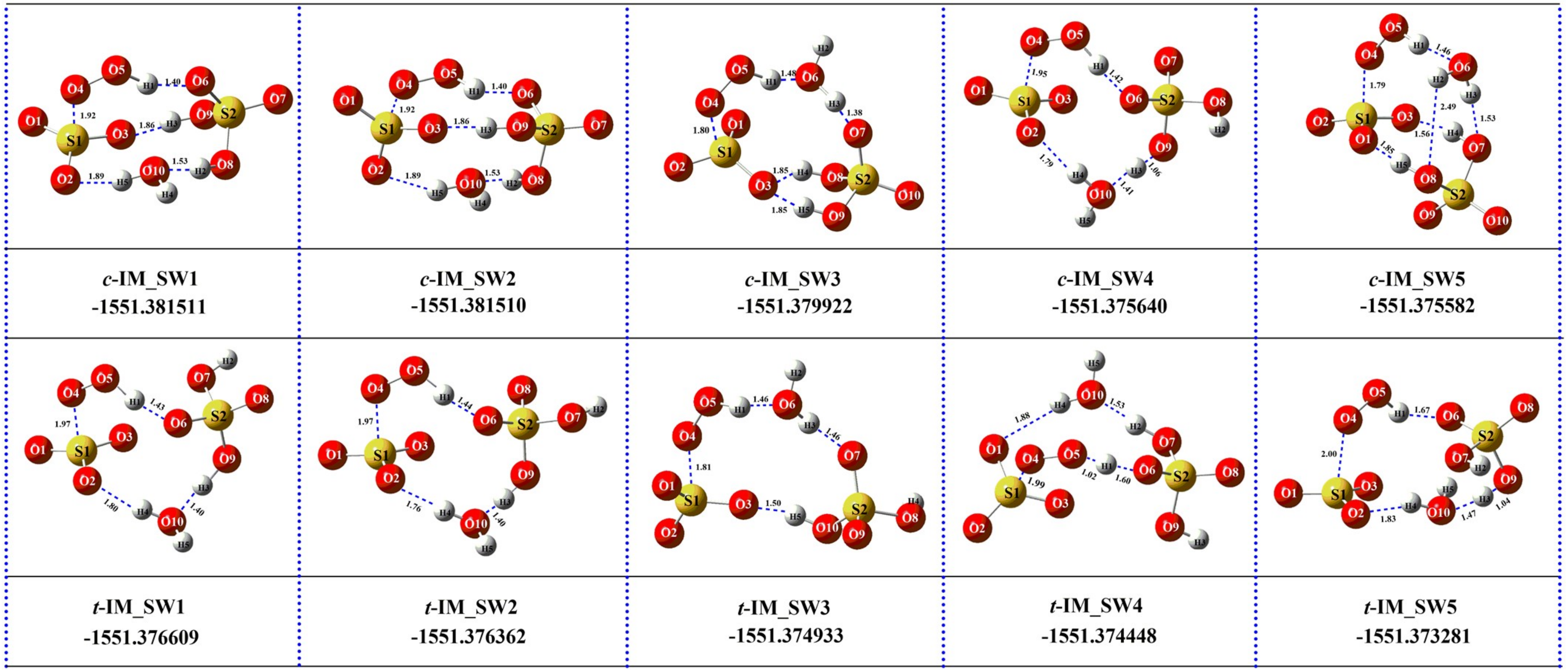

Fig. S4 The optimized geometries and electric energies (in Hartree-Fock) of $HO_2\cdots SO_3\cdots H_2SO_4\cdots H_2O$ at the M06-2X/6-311+G(2*df*,2*pd*) level of theory (Bond distances in Angstroms and angles in degrees)

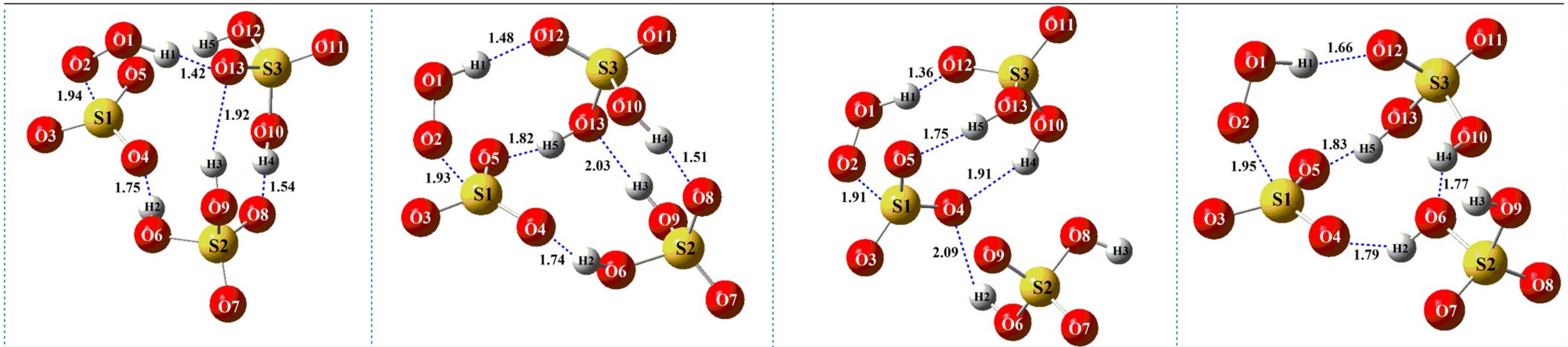

IM_SD1	IM_SD2	IM_SD3	IM_SD4
-2175.215926	-2175.213254	-2175.208702	-2175.208192

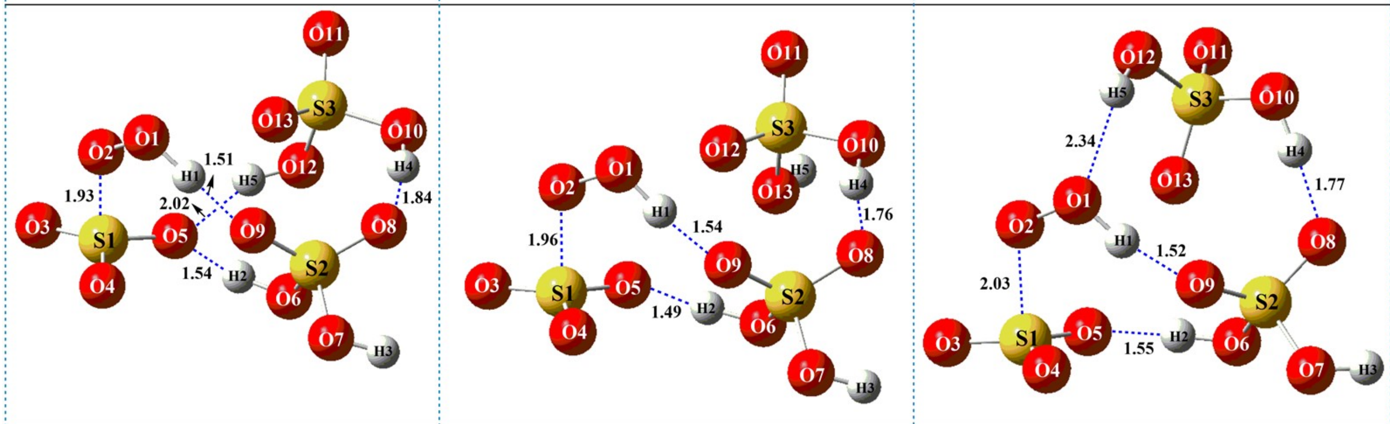

IM_SD5	IM_SD6	IM_SD7
-2175.207062	-2175.206528	-2175.203164

Fig. S5 The optimized geometries and electric energies (in Hartree-Fock) of $HO_2\cdots SO_3\cdots(H_2SO_4)_2$ at the M06-2X/6-311+G(2*df*,2*pd*) level of theory (Bond distances in Angstroms and angles in degrees)

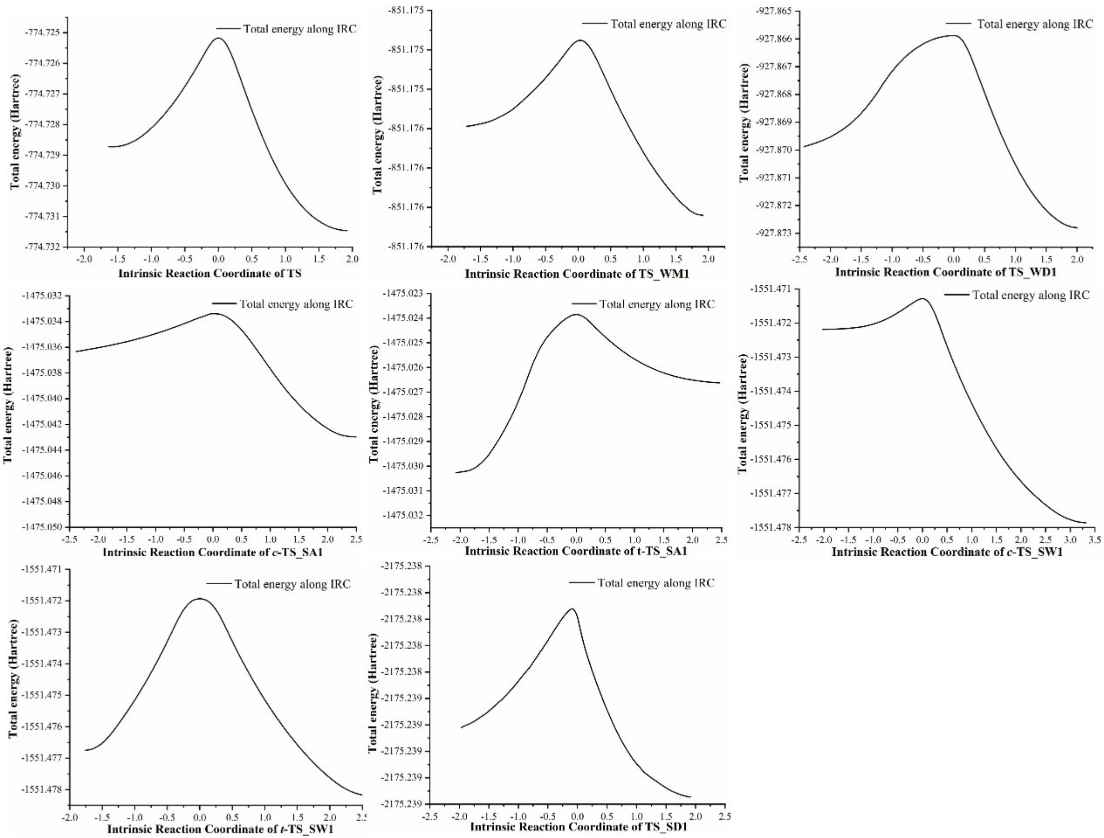

Fig. S6 The results of IRC calculations for all the transition states involved in the HO_2 + SO_3 reactions without and with catalyst *X* (*X* = H_2O, $(H_2O)_2$, H_2SO_4, $H_2SO_4{\cdots}H_2O$ and $(H_2SO_4)_2$)

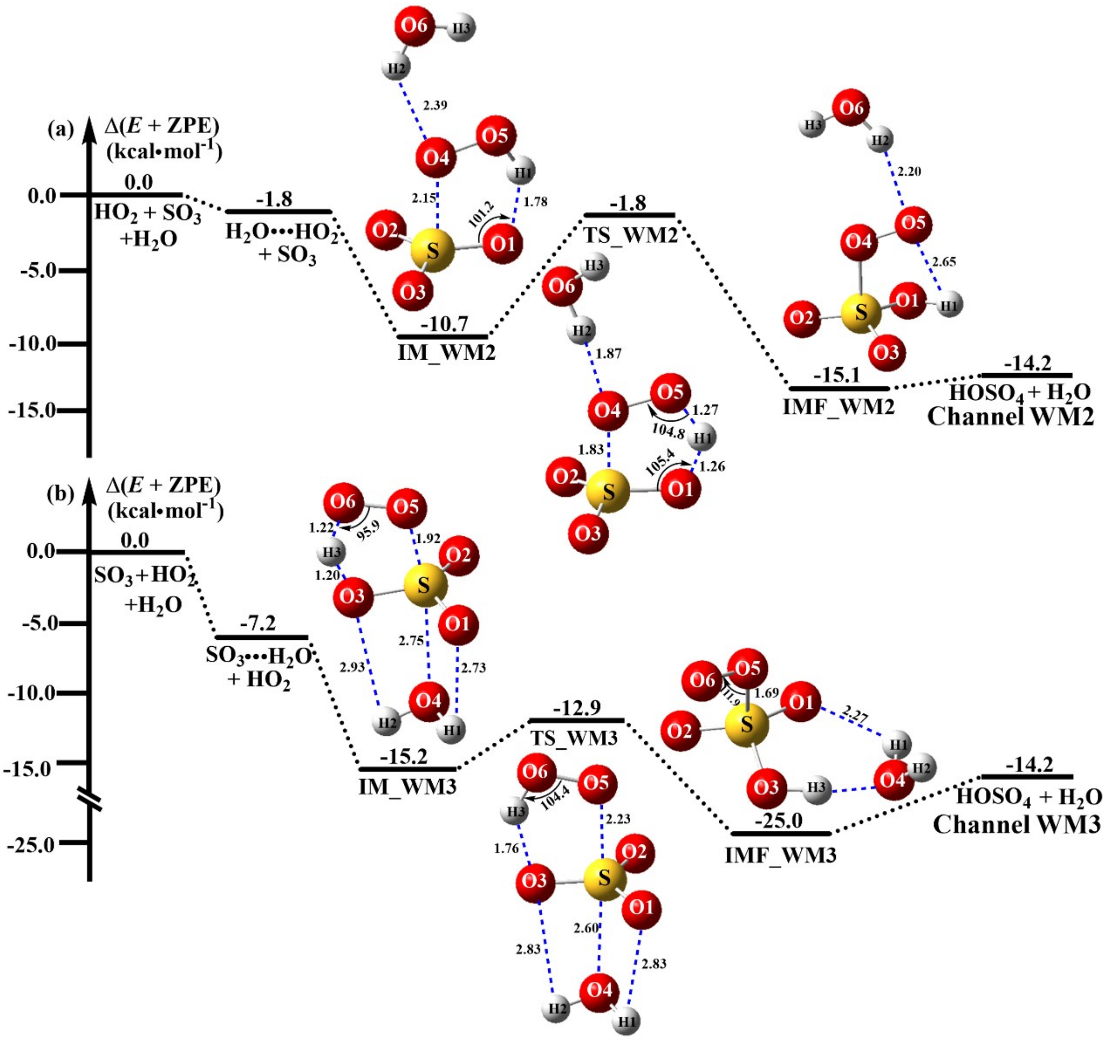

Fig. S7 Potential energy surface for the unfavorable routes in the HO_2 + SO_3 reaction with H_2O at the CCSD(T)/aug-cc-pVTZ//M06-2X/6-311+G(2*df*,2*pd*) level of theory

Table S2 The equilibrium constant (K_{eq}, in $cm^3 \cdot molecules^{-1}$)[a], and concentrations ($molecules \cdot cm^{-3}$) of complexes $HO_2 \cdots H_2O$, $SO_3 \cdots H_2O$, $H_2O \cdots HO_2$, $HO_2 \cdots (H_2O)_2$, $SO_3 \cdots (H_2O)_2$, *c*-$HO_2 \cdots H_2SO_4$, *c*-$SO_3 \cdots H_2SO_4$, *t*-$HO_2 \cdots H_2SO_4$, *t*-$SO_3 \cdots H_2SO_4$, *c*-$H_2SO_4 \cdots H_2O$, *c*-$HO_2 \cdots H_2SO_4 \cdots H_2O$, *c*-$SO_3 \cdots H_2SO_4 \cdots H_2O$, *t*-$H_2SO_4 \cdots H_2O$, *t*-$HO_2 \cdots H_2SO_4 \cdots H_2O$, *t*-$SO_3 \cdots H_2SO_4 \cdots H_2O$, $(H_2SO_4)_2$, $HO_2 \cdots (H_2SO_4)_2$ and $SO_3 \cdots (H_2SO_4)_2$ within the temperature range of 280-320 K

T/K	K_{eq1A}	[$HO_2 \cdots H_2O$]	K_{eq1B}	[$SO_3 \cdots H_2O$]	K_{eq1C}	[$H_2O \cdots HO_2$]
280	1.53×10^{-20}	1.18×10^{6}	1.73×10^{-20}	4.46	1.88×10^{-23}	1.45×10^{3}
290	9.42×10^{-21}	1.35×10^{6}	1.07×10^{-20}	5.12	1.68×10^{-23}	2.41×10^{3}
298	6.55×10^{-21}	1.52×10^{6}	7.50×10^{-21}	5.80	1.54×10^{-23}	3.58×10^{3}
300	6.00×10^{-21}	1.55×10^{6}	6.88×10^{-21}	5.90	1.51×10^{-23}	3.90×10^{3}
310	3.94×10^{-21}	1.73×10^{6}	4.55×10^{-21}	6.65	1.38×10^{-23}	6.03×10^{3}
320	2.66×10^{-21}	1.87×10^{6}	3.10×10^{-21}	7.28	1.26×10^{-23}	8.89×10^{3}
T/K	K_{eq2A}	[$HO_2 \cdots (H_2O)_2$]	K_{eq2B}	[$SO_3 \cdots (H_2O)_2$]	K_{eq3A}	[*c*-$HO_2 \cdots H_2SO_4$]
280	3.45×10^{-18}	2.11×10^{5}	1.10×10^{-17}	2.25	8.24×10^{-18}	9.64×10^{-1}
290	1.47×10^{-18}	2.60×10^{5}	4.80×10^{-18}	2.83	3.90×10^{-18}	4.45×10^{-1}
298	7.72×10^{-19}	3.15×10^{5}	2.57×10^{-18}	3.49	2.23×10^{-18}	2.47×10^{-1}
300	6.61×10^{-19}	3.21×10^{5}	2.21×10^{-18}	3.58	1.95×10^{-18}	2.10×10^{-1}
310	3.14×10^{-19}	3.82×10^{5}	1.07×10^{-18}	4.35	1.02×10^{-18}	1.07×10^{-1}
320	1.56×10^{-19}	4.32×10^{5}	5.44×10^{-19}	5.03	4.55×10^{-19}	4.64×10^{-2}
T/K	K_{eq3B}	[*c*-$SO_3 \cdots H_2SO_4$]	K_{eq4A}	[*t*-$HO_2 \cdots H_2SO_4$]	K_{eq4B}	[*t*-$SO_3 \cdots H_2SO_4$]
280	1.09×10^{-18}	4.25×10^{-7}	2.85×10^{-16}	3.33×10^{1}	3.09×10^{-19}	1.21×10^{-7}
290	5.13×10^{-19}	1.95×10^{-7}	1.19×10^{-16}	1.36×10^{1}	1.62×10^{-19}	6.17×10^{-8}
298	2.91×10^{-19}	1.08×10^{-7}	6.20×10^{-17}	6.89	1.00×10^{-19}	3.71×10^{-8}
300	2.54×10^{-19}	9.15×10^{-8}	5.30×10^{-17}	5.72	8.92×10^{-20}	3.21×10^{-8}
310	1.32×10^{-19}	4.62×10^{-8}	2.49×10^{-17}	2.61	5.11×10^{-20}	1.79×10^{-8}
320	7.16×10^{-20}	2.43×10^{-8}	1.22×10^{-17}	1.25	3.04×10^{-20}	1.03×10^{-8}
T/K	$K_{eq(c\text{-SW})}$	[*c*-$H_2SO_4 \cdots H_2O$]	K_{eq5A}	[*c*-$HO_2 \cdots H_2SO_4 \cdots H_2O$]	K_{eq5B}	[*c*-$SO_3 \cdots H_2SO_4 \cdots H_2O$]
280	2.03×10^{-19}	2.04×10^{7}	3.02×10^{-16}	1.85	5.30×10^{-19}	1.08×10^{-8}
290	1.20×10^{-19}	2.18×10^{7}	1.30×10^{-16}	8.53×10^{-1}	2.44×10^{-19}	5.33×10^{-9}
298	8.10×10^{-20}	2.31×10^{7} (2.40×10^{7})[b]	6.94×10^{-17}	4.80×10^{-1}	1.37×10^{-19}	3.16×10^{-9}
300	7.36×10^{-20}	2.27×10^{7}	5.96×10^{-17}	4.07×10^{-1}	1.19×10^{-19}	2.71×10^{-9}
310	4.67×10^{-20}	2.39×10^{7}	2.87×10^{-17}	2.05×10^{-1}	6.08×10^{-20}	1.45×10^{-9}
320	3.05×10^{-20}	2.44×10^{7}	1.45×10^{-17}	1.06×10^{-1}	3.24×10^{-20}	7.91×10^{-10}
T/K	$K_{eq(t\text{-SW})}$	[*t*-$H_2SO_4 \cdots H_2O$]	K_{eq6A}	[*t*-$HO_2 \cdots H_2SO_4 \cdots H_2O$]	K_{eq6B}	[*t*-$SO_3 \cdots H_2SO_4 \cdots H_2O$]
280	4.05×10^{-19}	4.08×10^{7}	2.20×10^{-15}	2.69×10^{1}	1.68×10^{-18}	3.43×10^{-8}
290	2.24×10^{-19}	4.07×10^{7}	9.24×10^{-16}	1.13×10^{1}	8.58×10^{-19}	1.87×10^{-8}
298	1.44×10^{-19}	4.09×10^{7}	4.82×10^{-16}	5.92	5.18×10^{-19}	1.20×10^{-8}
300	1.29×10^{-19}	3.99×10^{7}	4.12×10^{-16}	4.93	4.59×10^{-19}	1.04×10^{-8}
310	7.71×10^{-20}	3.94×10^{7}	1.94×10^{-16}	2.29	2.56×10^{-19}	6.11×10^{-9}
320	4.77×10^{-20}	3.81×10^{7}	9.58×10^{-17}	1.10	1.49×10^{-19}	3.63×10^{-9}

T/K	$K_{eq(SD)}$	$[(H_2SO_4)_2]$	K_{eq7A}	$[HO_2\cdots(H_2SO_4)_2]$	K_{eq7B}	$[SO_3\cdots(H_2SO_4)_2]$
280	4.88×10^{-17}	7.42	1.03×10^{-16}	2.29×10^{-7}	1.55×10^{-17}	1.15×10^{-13}
290	1.84×10^{-17}	2.65	4.36×10^{-17}	3.46×10^{-8}	6.96×10^{-18}	1.84×10^{-14}
298	8.82×10^{-18}	1.21	2.29×10^{-17}	8.31×10^{-9}	3.83×10^{-18}	4.63×10^{-15}
300	7.38×10^{-18}	1.01	1.96×10^{-17}	5.94×10^{-9}	3.31×10^{-18}	3.35×10^{-15}
310	3.15×10^{-18}	4.09×10^{-1}	9.30×10^{-18}	1.14×10^{-9}	1.66×10^{-18}	6.78×10^{-16}
320	1.42×10^{-18}	1.64×10^{-1}	4.63×10^{-18}	2.28×10^{-10}	8.69×10^{-19}	1.42×10^{-16}

[a] K_{eq1A}, K_{eq1B} and K_{eq1C} represented the equilibrium constant of $HO_2\cdots H_2O$, $SO_3\cdots H_2O$ and $H_2O\cdots HO_2$; K_{eq2A} and K_{eq2B} denoted the equilibrium constant of $HO_2\cdots(H_2O)_2$ and $SO_3\cdots(H_2O)_2$; K_{eq3A} and K_{eq3B} represented the equilibrium constant of c-$HO_2\cdots H_2SO_4$ and c-$SO_3\cdots H_2SO_4$; K_{eq4A} and K_{eq4B} denoted the equilibrium constant of t-$HO_2\cdots H_2SO_4$ and t-$SO_3\cdots H_2SO_4$; $K_{eq(c\text{-SW})}$, K_{eq5A} and K_{eq5B} denoted the equilibrium constant of c-$H_2SO_4\cdots H_2O$, c-$HO_2\cdots H_2SO_4\cdots H_2O$ and c-$SO_3\cdots H_2SO_4\cdots H_2O$; $K_{eq(t\text{-SW})}$, K_{eq6A} and K_{eq6B} represented the equilibrium constant of t-$H_2SO_4\cdots H_2O$, t-$HO_2\cdots H_2SO_4\cdots H_2O$ and t-$SO_3\cdots H_2SO_4\cdots H_2O$; $K_{eq(SD)}$, K_{eq7A} and K_{eq7B} denoted the equilibrium constant of $(H_2SO_4)_2$, $HO_2\cdots(H_2SO_4)_2$ and $SO_3\cdots(H_2SO_4)_2$.

[b] The concentrations of $HO_2\cdots H_2O$, $SO_3\cdots H_2O$ and $H_2O\cdots HO_2$ were respectively expressed as $[HO_2\cdots H_2O] = K_{eq1A} \times [H_2O] \times [HO_2]$, $[SO_3\cdots H_2O] = K_{eq1B} \times [H_2O] \times [SO_3]$ and $[H_2O\cdots HO_2] = K_{eq1C} \times [H_2O] \times [HO_2]$; the concentrations of $HO_2\cdots(H_2O)_2$ and $SO_3\cdots(H_2O)_2$ were respectively expressed as $[HO_2\cdots(H_2O)_2] = K_{eq2A} \times [(H_2O)_2] \times [HO_2]$ and $[SO_3\cdots(H_2O)_2] = K_{eq2B} \times [(H_2O)_2] \times [SO_3]$; the concentrations of c-$HO_2\cdots H_2SO_4$ and c-$SO_3\cdots H_2SO_4$ were respectively expressed as $[c\text{-}HO_2\cdots H_2SO_4] = K_{eq3A} \times [H_2SO_4] \times [HO_2]$ and $[c\text{-}SO_3\cdots H_2SO_4] = K_{eq3B} \times [H_2SO_4] \times [SO_3]$; the concentrations of t-$HO_2\cdots H_2SO_4$ and t-$SO_3\cdots H_2SO_4$ were respectively expressed as $[t\text{-}HO_2\cdots H_2SO_4] = K_{eq4A} \times [H_2SO_4] \times [HO_2]$ and $[t\text{-}SO_3\cdots H_2SO_4] = K_{eq4B} \times [H_2SO_4] \times [SO_3]$; the concentrations of c-$H_2SO_4\cdots H_2O$, c-$HO_2\cdots H_2SO_4\cdots H_2O$ and c-$SO_3\cdots H_2SO_4\cdots H_2O$ were respectively expressed as $[c\text{-}H_2SO_4\cdots H_2O] = K_{eq(c\text{-SW})} \times [H_2SO_4] \times [H_2O]$, $[c\text{-}HO_2\cdots H_2SO_4\cdots H_2O] = K_{eq5A} \times [H_2SO_4\cdots H_2O] \times [HO_2]$ and $[c\text{-}SO_3\cdots H_2SO_4\cdots H_2O] = K_{eq5B} \times [H_2SO_4\cdots H_2O] \times [SO_3]$; the concentrations of t-$H_2SO_4\cdots H_2O$, t-$HO_2\cdots H_2SO_4\cdots H_2O$ and t-$SO_3\cdots H_2SO_4\cdots H_2O$ were respectively expressed as $[t\text{-}H_2SO_4\cdots H_2O] = K_{eq(t\text{-SW})} \times [H_2SO_4] \times [H_2O]$, $[t\text{-}HO_2\cdots H_2SO_4\cdots H_2O] = K_{eq6A} \times [H_2SO_4\cdots H_2O] \times [HO_2]$ and $[t\text{-}SO_3\cdots H_2SO_4\cdots H_2O] = K_{eq6B} \times [H_2SO_4\cdots H_2O] \times [SO_3]$; the concentrations of $(H_2SO_4)_2$, $HO_2\cdots(H_2SO_4)_2$ and $SO_3\cdots(H_2SO_4)_2$ were respectively expressed as $[(H_2SO_4)_2] = K_{eq(SD)} \times [H_2SO_4]^2$, $[HO_2\cdots(H_2SO_4)_2] = K_{eq7A} \times [(H_2SO_4)_2] \times [HO_2]$ and $[SO_3\cdots(H_2SO_4)_2] = K_{eq7B} \times [(H_2SO_4)_2] \times [SO_3]$.

[c] The typical tropospheric concentrations [2,3] of 2.60×10^{17} - 2.30×10^{18} molecules·cm^{-3} for H_2O, 2.04×10^{14} - 9.24×10^{15} molecules·cm^{-3} for $(H_2O)_2$ and 5.0×10^{7} molecules·cm^{-3} of H_2SO_4 were respectively taken from reference. Besides, the concentrations of $H_2SO_4\cdots H_2O$ and $(H_2SO_4)_2$ were respectively calculated to be 2.04×10^{7} - 2.44×10^{7} molecules·cm^{-3} and 7.42×10^{0} - 1.64×10^{-1} molecules·cm^{-3}.

As for $HO_2\cdots X$ (X = H_2O, $(H_2O)_2$, H_2SO_4, $H_2SO_4\cdots H_2O$ and $(H_2SO_4)_2$) and $SO_3\cdots X$ complexes, their corresponding equilibrium constants and concentrations within the temperature range of 280-320 K have been listed in Table S2. However, due to the concentration [1,4] of SO_3 (1.0×10^{3} molecules·cm^{-3}) is much lower than that of HO_2 (3.0×10^{8} molecules·cm^{-3}), the concentrations of $HO_2\cdots X$ complexes shown in Table S2 are larger than those of $SO_3\cdots X$ complexes. Thus, we predict that the $HO_2 + SO_3$ rection in the presence of X mainly occurs through the $HO_2\cdots X + SO_3$ reaction.

Table S3 Zero point energy (ZPE/(kcal·mol^{-1})), entropies (S/(cal·mol^{-1}·K^{-1})), relative energies (ΔE and $\Delta(E$ + ZPE)/(kcal·mol^{-1})), enthalpies (ΔH(298)/(kcal·mol^{-1})) and free energies (ΔG(298)/(kcal·mol^{-1})) for the HO_2 + SO_3 reaction without and with catalyst X (X = H_2O, $(H_2O)_2$, H_2SO_4, H_2SO_4···H_2O and $(H_2SO_4)_2$)

Species	ZPE	ΔE	S	ΔG	$\Delta(E + \text{ZPE})$	ΔH	T_1
HO_2 + SO_3	16.3	0.0	115.8	0.0	0.0	0.0	0.0256; 0.0177
IM	18.6	-12.9	79.6	-9.8	-10.5	-11.2	0.0231
TS	16.5	-10.0	75.8	-8.6	-9.8	-11.1	0.0197
$HOSO_4$	18.6	-16.5	78.1	-13.1	-14.2	-15.0	0.0227
$HOSO_2$ + $^3O_2$	15.9	-2.6	48.9	12.8	-3.0	-2.9	0.0204, 0.0168
HO_2 + H_2O + SO_3	29.2	0.0	160.8	0.0	0.0	0.0	0.0256, 0.0106, 0.0177
HO_2···H_2O + SO_3	31.6	-9.2	132.3	1.0	-6.8	-7.5	0.0239, 0.0177
SO_3···H_2O + HO_2	31.5	-9.4	132.5	1.9	-7.2	-7.6	0.0163, 0.0256
IM_WM1	33.6	-23.9	90.2	0.2	-19.5	-20.9	0.0226
TS_WM1	32.6	-22.0	84.6	1.9	-18.5	-20.8	0.0245
IMF_WM1	33.7	-30.8	90.2	-6.7	-26.3	-27.8	0.0224
$HOSO_4$ + H_2O	31.5	-16.5	123.1	-3.7	-14.2	-15.0	0.0227, 0.0106
HO_2 + H_2O + SO_3	29.2	0.0	160.8	0.0	0.0	0.0	0.0256, 0.0106, 0.0177
H_2O···HO_2 + SO_3	30.7	-3.3	142.6	4.3	-1.8	-1.8	0.0235, 0.0177
IM_WM2	32.3	-13.9	104.3	5.9	-10.7	-11.0	0.0222
TS_WM2	30.8	-3.4	92.4	16.7	-1.8	-3.7	0.0242
IMF_WM2	32.8	-18.7	101.3	2.1	-15.1	-15.7	0.0222
$HOSO_4$ + H_2O	31.5	-16.5	123.2	-3.8	-14.2	-15.0	0.0227, 0.0106
HO_2 + H_2O + SO_3	29.2	0.0	160.8	0.0	0.0	29.2	0.0256, 0.0106, 0.0177
SO_3···H_2O + HO_2	31.5	-9.4	132.5	0.9	-7.0	31.5	0.0163, 0.0177
IM_WM3	32.8	-18.9	98.1	2.9	-15.2	32.8	0.0222
TS_WM3	30.7	-14.5	93.4	5.9	-12.9	30.7	0.0186
IMF_WM3	33.6	-29.4	91.9	-5.8	-25.0	33.6	0.0215
$HOSO_4$ + H_2O	31.5	-16.5	123.2	-3.8	-14.2	31.5	0.0227, 0.0106
HO_2 + $(H_2O)_2$ + SO_3	45.5	0.0	187.7	0.0	0.0	0.0	0.0256, 0.0123, 0.0177
HO_2···$(H_2O)_2$ + SO_3	48.8	-15.9	147.1	-1.9	-12.6	-14.0	0.0240, 0.0256
SO_3···$(H_2O)_2$+ HO_2	48.4	-16.5	146.6	-2.3	-13.6	-14.6	0.0233, 0.0177
IM_WD1	49.4	-28.6	108.0	-2.5	-24.6	-26.2	0.0224
TS_WD1	48.3	-27.9	91.5	-1.9	-25.2	-27.5	0.0240
IMF_WD1	50.3	-35.0	106.9	-7.5	-30.2	-32.2	0.0212
$HOSO_4$ + $(H_2O)_2$	31.5	-16.5	123.2	-3.8	-14.2	31.5	0.0227, 0.0123
HO_2 + c-H_2SO_4 + SO_3	40.0	0.0	188.2	0.0	0.0	0.0	0.0256, 0.0161, 0.0177
c-HO_2···H_2SO_4 + SO_3	41.8	-15.1	152.1	-3.1	-13.4	-13.9	0.0225, 0.0177

c- $SO_3\cdots H_2SO_4$ + HO_2	41.5	-13.6	148.5	-0.8	-12.2	-12.6	0.0169, 0.0256
c-IM_SA1	42.6	-26.4	109.0	-1.2	-23.8	-24.8	0.0175
c-TS_SA1	41.5	-24.9	105.2	-0.4	-23.5	-25.1	0.0205
c-IMF_SA1	43.3	-32.8	108.1	-6.7	-29.5	-30.6	0.0219
$HOSO_4$ + *c*-H_2SO_4	42.4	-16.5	150.6	-3.8	-14.2	-15.0	0.0227, 0.0161
HO_2 + *t*-H_2SO_4 + SO_3	40.3	0.0	189.5	0.0	0.0	0.0	0.0256, 0.0162, 0.0177
t-$HO_2\cdots H_2SO_4$ + SO_3	41.7	-15.5	153.9	-3.9	-14.1	-14.5	0.0225, 0.0177
t-$SO_3\cdots H_2SO_4$ + HO_2	41.3	-12.1	154.6	-0.4	-11.1	-10.8	0.0169, 0.0256
t-IM_SA1	42.8	-23.8	111.1	1.5	-21.3	-21.9	0.0198
t-TS_SA1	40.2	-18.3	106.6	4.9	-18.4	-19.8	0.0207
t-IMF_SA1	42.8	-27.1	111.8	-7.1	-24.6	-30.3	0.0222
$HOSO_4$ + *t*-H_2SO_4	42.4	-16.5	149.7	-3.8	-14.2	-15.0	0.0227, 0.0162
HO_2 + *c*-$H_2SO_4\cdots H_2O$ + SO_3	55.2	0.0	202.5	0.0	0.0	0.0	0.0256, 0.0148, 0.0177
c-$HO_2\cdots H_2SO_4\cdots H_2O$ + SO_3	56.5	-15.0	166.6	-3.3	-13.6	-14.1	0.0213, 0.0177
c-$SO_3\cdots H_2SO_4\cdots H_2O$ + HO_2	59.6	-17.0	156.8	-2.3	-12.5	-13.3	0.0162, 0.0256
c-IM_SW1	57.6	-28.0	119.8	-2.0	-25.6	-26.6	0.0192
c-TS_SW1	56.3	-26.5	117.6	-1.5	-25.3	-26.8	0.0174
c-IMF_SW1	57.8	-33.4	122.3	-7.9	-30.8	-31.8	0.0209
$HOSO_4$ + *c*-$H_2SO_4\cdots H_2O$	57.5	-16.5	164.9	-3.8	-14.2	-15.0	0.0227, 0.0148
HO_2 + *t*-$H_2SO_4\cdots H_2O$ + SO_3	55.4	0.0	200.6	0.0	0.0	0.0	0.0256, 0.0153, 0.0177
t-$HO_2\cdots H_2SO_4\cdots H_2O$ + SO_3	56.5	-15.3	167.2	-4.5	-14.2	-14.4	0.0213; 0.0177
t- $SO_3\cdots H_2SO_4\cdots H_2O$ + HO_2	55.8	-11.9	166.5	-1.1	-11.5	-11.3	0.0162, 0.0256
t-IM_SW1	57.3	-24.8	125.8	-1.2	-22.9	-23.5	0.0192
t-TS_SW1	54.9	-21.4	118.6	1.2	-21.8	-23.3	0.0174
t-IMF_SW1	57.4	-32.6	124.3	-8.7	-30.6	-31.4	0.0209
$HOSO_4$ + *t*-$H_2SO_4\cdots H_2O$	57.7	-16.5	162.9	-3.8	-14.2	-15.0	0.0227, 0.0153
HO_2 + $(H_2SO_4)_2$ + SO_3	65.1	0.0	224.0	0.0	0.0	0.0	0.0256, 0.0181, 0.0177
$HO_2\cdots(H_2SO_4)_2$ + SO_3	66.7	-15.7	184.0	-2.5	-14.0	-14.4	0.0218, 0.0177
$SO_3\cdots(H_2SO_4)_2$ + HO_2	57.2	-14.1	126.8	-0.8	-13.2	-13.4	0.0157, 0.0256
IM_SD1	67.7	-31.8	140.0	-5.0	-26.0	-30.0	0.0183
TS_SD1	65.8	-32.0	136.2	-6.4	-27.0	-32.7	0.0205
IMF_SD1	67.5	-36.3	139.5	-9.6	-31.3	-34.7	0.0215
$HOSO_4$ + $(H_2SO_4)_2$	67.4	-16.5	184.1	-3.8	-14.2	-15.0	0.0227, 0.0181

<table>
<tr><th>Species</th><th>Potential energy surfaces for the internal rotations</th></tr>
<tr><td>$HO_2 \cdots SO_3$ (IM)</td><td>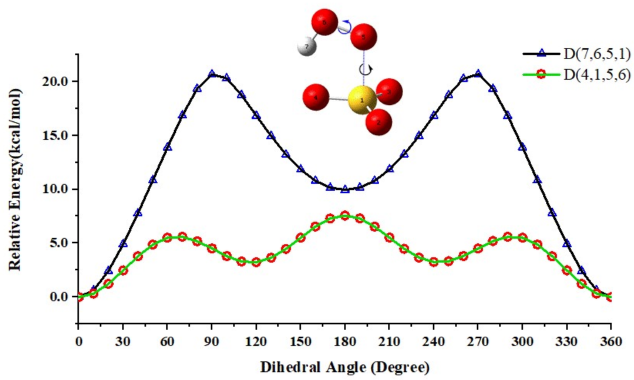
</td></tr>
<tr><td>$HOSO_4$ (IMF)</td><td>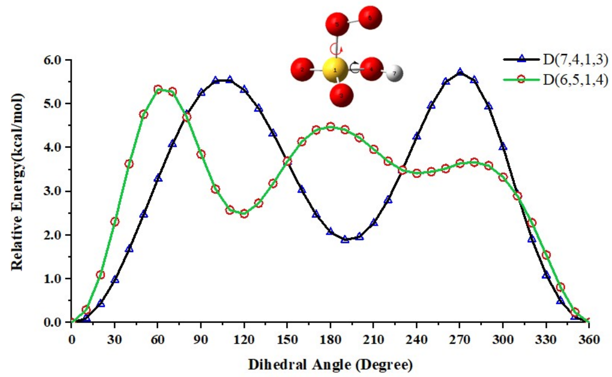
</td></tr>
<tr><td>$HOSO_2$</td><td>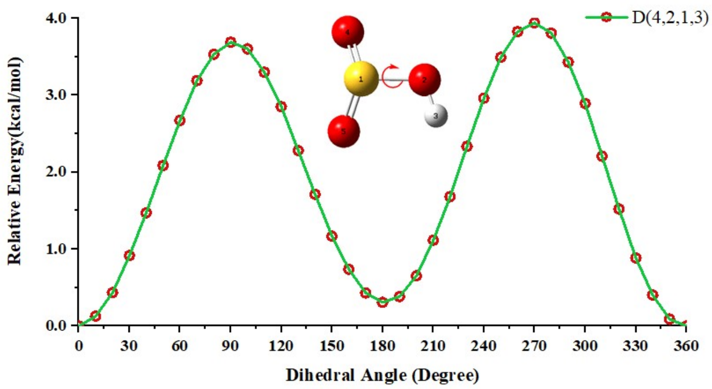
</td></tr>
</table>

Fig. S8 Hindrance potentials for $HO_2 \cdots SO_3$, $HOSO_4$ and $HOSO_2$ calculated at the M06-2X/6-311+G(2*df*,2*pd*) level of theory

For hindered internal rotation (HIR) treatment, the hindrance potentials, $V(\theta)$, as a function of torsional angle, θ, along with the single bonds (i.e., S1-O4 and O4-O5, Fig. S8) were explicitly obtained at the M06-2X/6-311+G(2*df*,2*pd*) level via relaxed surface scans with the step size of 10° for the dihedral angles corresponding to the rotations. As seen in Fig. S8, the single bond of O4-O5 and S1-O4 in $HO_2 \cdots SO_3$, the single bond of S1-O4 in $HOSO_4$ and the single bond of S1-O4 in $HOSO_2$ need to treated by hindered internal rotators. The parameters of the HIR are automatically determined using the Graphical User Interface (GUI) in Mesmer software, and the procedural details of the hindered internal rotation (HIR) correction can be found in the works of Le et al.[5,6] and Mai et al.[7-14]

Part A Hindered internal rotation analysis for the HO_2 + SO_3 reaction without and with *X* (*X* = H_2O, $(H_2O)_2$, H_2SO_4, $H_2SO_4\cdots H_2O$ and $(H_2SO_4)_2$)

Within the temperature range of 280-320 K, the rate constants (k_{R1}) for the HO_2 + SO_3 reaction without and with HIR treatments at 760 Torr has been listed in Table S4. It should be noted that, at 760 Torr, the HIR correction just plays a minor role in the HO_2 + SO_3 reaction, e.g., HIR treatment listed in Table S4 enhanced the rate constants by a factor of 1.14 to 1.15 within the temperature range of 280-320 K. Besides, the hindered internal rotation analysis for the pre- and post-reactive complexes and transition states involved in the HO_2 + SO_3 reaction with *X* have been calculated in the Gaussian 09 program with the keywords of "freq = hindrot" and "integral = ultrafine". The calculations reveal that no frequencies need to be corrected. So, we predict that the HIR correction just plays a minor role in the HO_2 + SO_3 reaction with *X*. This can be explained by two reasons as follows. On the one hand, the pre- and post-reactive complexes and transition states involved in the HO_2 + SO_3 reaction with *X* were shown the quasi-planar ring structures and cage-like ring structures. As compared with the naked reaction (Fig. 3(a)), these ring structures reduce the ring tension obviously and increase the stability of the pre- and post-reactive complex and transition state greatly. On the other hand, the numbers of hydrogen bonds in *X*-assisted pre- and post-reactive complexes and transition states were increased, which hinder the rotation bonds of S-O4 and O4-O5 (Fig. 3-6) in *X*-assisted pre- and post-reactive complex and transition state. The detail information for the rate constants (k_{R1}) for the HO_2 + SO_3 reaction without and with HIR treatments has been displayed in Table S4.

Table S4 The rate constants (k_{R1}) for the HO_2 + SO_3 reaction without and with HIR treatments within the temperature range of 280-320 K (at 760 Torr)

with HIR treatments	without HIR treatments	Factor
2.11×10^{-11}	1.85×10^{-11}	1.14
1.95×10^{-11}	1.71×10^{-11}	1.14
1.83×10^{-11}	1.60×10^{-11}	1.14
1.80×10^{-11}	1.57×10^{-11}	1.14
1.66×10^{-11}	1.45×10^{-11}	1.15
1.53×10^{-11}	1.33×10^{-11}	1.15

Table S5 The calculated branching ratio (β)[a] for the three pathways ($HO_2\cdots SO_3\cdots X \rightarrow HOSO_2 + O_2 + X$, path 1, $HO_2\cdots SO_3\cdots X \rightarrow HO_2 + SO_3\cdots X$, path 2, and $HO_2\cdots SO_3\cdots X \rightarrow HO_2\cdots X + SO_3$, path 3) yielding from $HO_2\cdots SO_3\cdots X$ adduct within the pressure range of 10-300 Torr (at 298 K)

P (Torr)	Branching Ratio (%) for $HO_2\cdots SO_3\cdots X$ complex											
	$HO_2\cdots SO_3$		$HO_2\cdots SO_3\cdots H_2O$		$HO_2\cdots SO_3\cdots (H_2O)_2$		$HO_2\cdots SO_3\cdots H_2SO_4$		$HO_2\cdots SO_3\cdots H_2SO_4\cdots H_2O$		$HO_2\cdots SO_3\cdots (H_2SO_4)_2$	
	β_1	$\beta_2+\beta_3$	β_1	$\beta_2+\beta_3$	β_1	$\beta_2+\beta_3$	β_1	$\beta_2+\beta_3$	β_1	$\beta_2+\beta_3$	β_1	$\beta_2+\beta_3$
300	99.89%	0.11%	99.85%	0.15%	99.97%	0.03%	99.93%	0.07%	99.93%	0.07%	99.88%	0.12%
100	99.84%	0.16%	99.86%	0.14%	99.98%	0.02%	99.95%	0.05%	99.95%	0.05%	99.95%	0.05%
50	99.80%	0.20%	99.87%	0.13%	99.98%	0.02%	99.96%	0.04%	99.96%	0.04%	99.96%	0.04%
10	99.76%	0.24%	99.87%	0.13%	99.99%	0.01%	99.97%	0.03%	99.97%	0.03%	99.98%	0.02%

[a] β_1, β_2 and β_3 were the branching ratio for the path 1, path 2 and path 3. The calculated β_1, β_2 and β_3 can be respectively expressed as $\beta_1 = k_{path\ 1}/(k_{path\ 1} + k_{path\ 2} + k_{path\ 3})$, $\beta_2 = k_{path\ 2}/(k_{path\ 1} + k_{path\ 2} + k_{path\ 3})$ and $\beta_3 = k_{path\ 3}/(k_{path\ 1} + k_{path\ 2} + k_{path\ 3})$.

The pressure dependent rate constant for the three pathways ($HO_2\cdots SO_3\cdots X \rightarrow HOSO_2 + O_2 + X$, path 1, $HO_2\cdots SO_3\cdots X \rightarrow HO_2 + SO_3\cdots X$, path 2, and $HO_2\cdots SO_3\cdots X \rightarrow HO_2\cdots X + SO_3$, path 3) yielding from $HO_2\cdots SO_3\cdots X$ adduct as given below,

$$HO_2\cdots SO_3\cdots X \rightarrow HOSO_2 + O_2 + X \quad \text{(path 1)}$$

$$HO_2\cdots SO_3\cdots X \rightarrow HO_2 + SO_3\cdots X \quad \text{(path 2)}$$

$$HO_2\cdots SO_3\cdots X \rightarrow HO_2\cdots X + SO_3 \quad \text{(path 3)}$$

The pressure dependent rate constant at 298 K for the above-mentioned pathways were calculated within the pressure range of 10-300 Torr. Their corresponding branching ratios were given in Table S5. As can be seen from Table S5, one can easily conclude that path 1 was the major pathway, whereas paths 2 and 3 were the minor channels within the pressure range of 10-300 Torr. Since the branching ratios of path 1 were more than 99%, the paths 2 and 3 can be conveniently avoided for further discussion. The result and discussion will be based on the kinetics of path 1 only unless otherwise stated.

Part B Bimolecular rate constants ($cm^3 \cdot molecules^{-1} \cdot s^{-1}$) for the SO_3 + $HO_2 \cdots X$ (X = H_2O, $(H_2O)_2$, H_2SO_4, $H_2SO_4 \cdots H_2O$ and $(H_2SO_4)_2$) and HO_2 + $SO_3 \cdots X$ reactions

As for the $HO_2 + SO_3 + X$ ($X = H_2O$, $(H_2O)_2$, H_2SO_4, $H_2SO_4 \cdots H_2O$ and $(H_2SO_4)_2$) reaction, two entry channels $HO_2 \cdots X + SO_3$ (Channel A) and $SO_3 \cdots X + HO_2$ (Channel B) have been considered for the rate constants calculations as follows.

Channel A

$$\text{Step 1A: } HO_2 + X \underset{k_{-1A}}{\overset{k_{1A}}{\rightleftharpoons}} HO_2 \cdots X \quad (S1)$$

$$\text{Step 2A: } HO_2 \cdots X + SO_3 \underset{k_{-2A}}{\overset{k_{2A}}{\rightleftharpoons}} \text{products} \quad (S2)$$

Channel B

$$\text{Step 1B: } SO_3 + X \underset{k_{-1B}}{\overset{k_{1B}}{\rightleftharpoons}} SO_3 \cdots X \quad (S3)$$

$$\text{Step 2B: } SO_3 \cdots X + HO_2 \underset{k_{-2B}}{\overset{k_{2B}}{\rightleftharpoons}} \text{products} \quad (S4)$$

As for the $HO_2 + SO_3 + X$ reaction, two entry channels $HO_2 \cdots X + SO_3$ (Channel A) and $SO_3 \cdots X$ + HO_2 (Channel B) have been respectively considered for the rate constants calculations involved in Table S6 and Table S7. Due to the fact that both of the $HO_2 \cdots X + SO_3$ and $SO_3 \cdots X + HO_2$ reactions proceed through the same pre-reactive trimolecular complex $HO_2 \cdots SO_3 \cdots X$, so the product of $K_{eq1A} \times k_{2A}$ is equal to the product of $K_{eq1B} \times k_{2B}$. Based on two facts above, the effective rate constant for the $HO_2 \cdots X + SO_3$ reaction was equal to the $SO_3 \cdots X + HO_2$ reaction. These results have been reported in our previous work [15,16]. The detail information of bimolecular rate constants ($cm^3 \cdot molecules^{-1} \cdot s^{-1}$) for the $SO_3 + HO_2 \cdots X$ ($X = H_2O$, $(H_2O)_2$, H_2SO_4, $H_2SO_4 \cdots H_2O$ and $(H_2SO_4)_2$) and HO_2 + $SO_3 \cdots X$ reaction have been respectively listed in Table 1 and Table S6.

Table S6 Bimolecular rate constants ($cm^3 \cdot molecules^{-1} \cdot s^{-1}$) for the $HO_2 + SO_3 \cdots X$ ($X = H_2O$, $(H_2O)_2$, H_2SO_4, $H_2SO_4 \cdots H_2O$ and $(H_2SO_4)_2$) reaction calculated by master equation within the temperature range of 280-320 K (at 760 Torr) [a]

Reaction	T (K)	280	290	298	300	310	320
Channel WM1	k_{WM1_b}	1.61×10^{-11}	1.34×10^{-11}	1.16×10^{-11}	1.12×10^{-11}	9.25×10^{-12}	7.65×10^{-12}
Channel WD1	k_{WD1_b}	1.15×10^{-11}	8.75×10^{-12}	7.01×10^{-12}	6.63×10^{-12}	5.01×10^{-12}	3.77×10^{-12}
Channel *c*-SA	$k_{c\text{-SA\_b}}$	2.05×10^{-11}	1.57×10^{-11}	1.26×10^{-11}	1.20×10^{-11}	9.06×10^{-11}	6.84×10^{-11}
Channel *t*-SA	$k_{t\text{-SA\_b}}$	1.77×10^{-13}	1.25×10^{-13}	9.41×10^{-14}	8.77×10^{-14}	6.18×10^{-14}	4.37×10^{-14}
Channel *c*-SW	$k_{c\text{-SW\_b}}$	6.06×10^{-11}	5.09×10^{-11}	4.38×10^{-11}	4.21×10^{-11}	3.45×10^{-11}	2.79×10^{-11}
Channel *t*-SW	$k_{t\text{-SW\_b}}$	7.18×10^{-12}	5.61×10^{-12}	4.60×10^{-12}	4.37×10^{-12}	3.39×10^{-12}	2.62×10^{-12}
Channel SD	k_{SD_b}	6.59×10^{-11}	5.40×10^{-11}	4.55×10^{-11}	4.35×10^{-11}	3.44×10^{-11}	2.68×10^{-11}

k_{WM1_b}, k_{WD1_b}, $k_{c\text{-SA\_b}}$, $k_{t\text{-SA\_b}}$, $k_{c\text{-SW\_b}}$, $k_{t\text{-SW\_b}}$ and k_{SD_b} was respectively denoted the rate constants for the $HO_2 + SO_3 \cdots H_2O$, $HO_2 + SO_3 \cdots (H_2O)_2$, HO_2 + *c*-$SO_3 \cdots H_2SO_4$, HO_2 + *t*-$SO_3 \cdots H_2SO_4$, HO_2 + *c*-$SO_3 \cdots H_2SO_4 \cdots H_2O$, HO_2 + *t*-$SO_3 \cdots H_2SO_4 \cdots H_2O$ and HO_2 + *c*-$SO_3 \cdots (H_2SO_4)_2$ reactions.

Table S7 The calculated rate constants ($cm^3 \cdot molecules^{-1} \cdot s^{-1}$) for the HO_2 + SO_3 reaction without and with H_2O, $(H_2O)_2$ and H_2SO_4 within the temperature range of 280-320 K and the pressure range of 10-760 Torr

	T(K)	10 Torr	50 Torr	100 Torr	300 Torr	760 Torr
k_{R1}	280	2.11×10^{-11}	2.11×10^{-11}	2.11×10^{-11}	2.11×10^{-11}	2.11×10^{-11}
	290	1.95×10^{-11}	1.95×10^{-11}	1.95×10^{-11}	1.95×10^{-11}	1.95×10^{-11}
	298	1.8×10^{-11}	1.83×10^{-11}	1.83×10^{-11}	1.83×10^{-11}	1.83×10^{-11}
	300	1.80×10^{-11}	1.80×10^{-11}	1.80×10^{-11}	1.80×10^{-11}	1.80×10^{-11}
	310	1.66×10^{-11}	1.66×10^{-11}	1.66×10^{-11}	1.66×10^{-11}	1.66×10^{-11}
	320	1.53×10^{-11}	1.53×10^{-11}	1.53×10^{-11}	1.53×10^{-11}	1.53×10^{-11}
k_{WM1}	280	1.63×10^{-11}	1.64×10^{-11}	1.64×10^{-11}	1.64×10^{-11}	1.65×10^{-11}
	290	1.39×10^{-11}	1.40×10^{-11}	1.40×10^{-11}	1.40×10^{-11}	1.40×10^{-11}
	298	1.21×10^{-11}	1.22×10^{-11}	1.22×10^{-11}	1.22×10^{-11}	1.22×10^{-11}
	300	1.17×10^{-11}	1.18×10^{-11}	1.18×10^{-11}	1.18×10^{-11}	1.18×10^{-11}
	310	9.82×10^{-12}	9.95×10^{-12}	9.97×10^{-12}	9.98×10^{-12}	9.99×10^{-12}
	320	8.22×10^{-12}	8.38×10^{-12}	8.40×10^{-12}	8.41×10^{-12}	8.42×10^{-12}
k_{WD}	280	4.77×10^{-11}	4.81×10^{-11}	4.81×10^{-11}	4.82×10^{-11}	4.82×10^{-11}
	290	4.18×10^{-11}	4.23×10^{-11}	4.23×10^{-11}	4.24×10^{-11}	4.24×10^{-11}
	298	3.74×10^{-11}	3.79×10^{-11}	3.79×10^{-11}	3.80×10^{-11}	3.80×10^{-11}
	300	3.63×10^{-11}	3.68×10^{-11}	3.68×10^{-11}	3.69×10^{-11}	3.69×10^{-11}
	310	3.13×10^{-11}	3.18×10^{-11}	3.18×10^{-11}	3.19×10^{-11}	3.19×10^{-11}
	320	2.76×10^{-11}	2.80×10^{-11}	2.80×10^{-11}	2.84×10^{-11}	2.84×10^{-11}
$k_{c\text{-SA}}$	280	1.48×10^{-11}	1.60×10^{-11}	1.62×10^{-11}	1.63×10^{-11}	1.64×10^{-11}
	290	1.19×10^{-11}	1.28×10^{-11}	1.30×10^{-11}	1.31×10^{-11}	1.31×10^{-11}
	298	8.50×10^{-12}	1.03×10^{-11}	1.06×10^{-11}	1.08×10^{-11}	1.09×10^{-11}
	300	7.89×10^{-12}	9.76×10^{-12}	1.01×10^{-11}	1.03×10^{-11}	1.04×10^{-11}
	310	5.13×10^{-12}	7.22×10^{-12}	7.66×10^{-12}	8.00×10^{-12}	8.18×10^{-12}
	320	3.69×10^{-12}	4.50×10^{-12}	5.47×10^{-12}	5.66×10^{-12}	6.40×10^{-12}

Table S8 Effective rate constants (k') for the $HO_2 + SO_3$ reaction with X ($X = H_2O$, $(H_2O)_2$, H_2SO_4, $H_2SO_4 \cdots H_2O$ and $(H_2SO_4)_2$) within the temperature range of 280-320 K (at 0 km altitude)

Channels	T (K)	280	290	298	300	310	320
Channel WM1	k'_{WM1}	6.48×10^{-14}	6.28×10^{-14}	6.10×10^{-14}	6.09×10^{-14}	5.75×10^{-14}	5.26×10^{-14}
Channel WM2	k'_{WM2}	5.92×10^{-21}	8.51×10^{-21}	1.13×10^{-20}	1.20×10^{-20}	1.65×10^{-20}	2.16×10^{-20}
Channel WM3	k'_{WM3}	3.33×10^{-14}	3.09×10^{-14}	2.96×10^{-14}	2.89×10^{-14}	2.62×10^{-14}	2.32×10^{-14}
Channel WD1	k'_{WD1}	3.39×10^{-14}	3.68×10^{-14}	3.80×10^{-14}	3.96×10^{-14}	4.06×10^{-14}	4.11×10^{-14}
Channel *c*-SA	$k'_{c\text{-SA}}$	5.27×10^{-20}	1.94×10^{-20}	8.98×10^{-21}	7.29×10^{-21}	2.92×10^{-21}	9.91×10^{-22}
Channel *t*-SA	$k'_{t\text{-SA}}$	1.23×10^{-20}	3.49×10^{-21}	1.53×10^{-21}	1.21×10^{-21}	4.89×10^{-22}	1.53×10^{-22}
Channel *c*-SW	$k'_{c\text{-SW}}$	1.05×10^{-19}	4.00×10^{-20}	1.92×10^{-20}	1.56×10^{-20}	6.38×10^{-21}	2.63×10^{-21}
Channel *t*-SW	$k'_{t\text{-SW}}$	5.02×10^{-19}	1.68×10^{-19}	7.38×10^{-20}	5.87×10^{-20}	2.18×10^{-20}	8.30×10^{-21}
Channel SD	k'_{SD}	2.85×10^{-26}	3.82×10^{-27}	8.20×10^{-28}	5.69×10^{-28}	9.36×10^{-29}	1.57×10^{-29}
k'_{WM1}/k_{tot} (%)		0.31%	0.32%	0.33%	0.34%	0.34%	0.34%
k'_{WD1}/k_{tot} (%)		0.16%	0.19%	0.21%	0.22%	0.24%	0.27%

Table S9 Equilibrium constants (K_{eq}, cm^3·$molecules^{-1}$) for the formation of $HO_2\cdots H_2O$, $HO_2\cdots(H_2O)_2$, *c*-$HO_2\cdots H_2SO_4$ and *c*-$HO_2\cdots H_2SO_4\cdots H_2O$ complexes, concentrations (molecules·cm^{-3}) of H_2O, $(H_2O)_2$, H_2SO_4 and $H_2SO_4\cdots H_2O$, and rate constants (cm^3·$molecules^{-1}$·s^{-1}) of the HO_2 + SO_3 reaction with H_2O, $(H_2O)_2$, H_2SO_4 and $H_2SO_4\cdots H_2O$ at different altitudes in troposphere

Altitude	T(K)	P(atm)	k_{WM1}	$K_{eq}(HO_2\cdots H_2O)$	$[H_2O]$
5 km	259.3	0.535	1.22×10^{-11}	3.26×10^{-20}	2.41×10^{16}
10 km	229.7	0.266	2.85×10^{-11}	2.83×10^{-19}	4.92×10^{15}
15 km	212.6	0.120	2.26×10^{-11}	1.18×10^{-18}	1.96×10^{13}
Altitude	T(K)	P(atm)	k_{WD1}	$K_{eq}(HO_2\cdots(H_2O)_2)$	$[(H_2O)_2]$
5 km	259.3	0.535	6.64×10^{-12}	2.56×10^{-17}	2.70×10^{12}
10 km	229.7	0.266	4.20×10^{-11}	7.39×10^{-16}	2.30×10^{11}
15 km	212.6	0.120	6.02×10^{-11}	8.06×10^{-15}	6.30×10^{6}
Altitude	T(K)	P(atm)	$k_{c\text{-SA}}$	$K_{eq}(c\text{-}HO_2\cdots H_2SO_4)$	$[H_2SO_4]$
5 km	259.3	0.535	2.68×10^{-11}	4.81×10^{-17}	6.00×10^{7}
10 km	229.7	0.266	2.63×10^{-11}	9.49×10^{-16}	8.30×10^{6}
15 km	212.6	0.120	1.90×10^{-11}	8.03×10^{-15}	2.40×10^{5}
Altitude	T(K)	P(atm)	$k_{c\text{-SW}}$	$K_{eq}(c\text{-}HO_2\cdots H_2SO_4\cdots H_2O)$	$[H_2SO_4\cdots H_2O]$[a]
5 km	259.3	0.535	3.45×10^{-11}	9.79×10^{-17}	1.02×10^{6}
10 km	229.7	0.266	3.54×10^{-11}	1.88×10^{-15}	2.34×10^{5}
15 km	212.6	0.120	2.42×10^{-11}	1.56×10^{-14}	1.21×10^{2}

[a] The concentrations of $H_2SO_4\cdots H_2O$ at 5, 10 and 15 km altitudes were respectively calculated to be 1.02×10^5, 2.34×10^5 and 1.21×10^2 molecules·cm^{-3} by using the above concentration of H_2SO_4 and H_2O.

The average concentration[2,17] of H_2SO_4 at 5, 10 and 15 km altitudes were known to be 6.00×10^7, 8.30×10^6 and 2.40×10^5 molecules·cm^{-3}, respectively. Meanwhile, the concentration for H_2O was respectively found to be 2.41×10^{16}, 4.92×10^{15} and 1.96×10^{13} molecules·cm^{-3}, whereas the concentration of $(H_2O)_2$ was respectively found to be 2.70×10^{12}, 2.30×10^{11} and 6.30×10^6 molecules·cm^3, in the same order considering temperatures (259 K, 230 K and 213 K, respectively) and pressures (0.533, 0.266 and 0.120 atm, respectively) at those altitudes (Table S9). Using the above concentrations of H_2SO_4 and H_2O along with the equilibrium constants for the $H_2SO_4\cdots H_2O$ complex formation, the concentrations of $H_2SO_4\cdots H_2O$ complex were calculated to be 1.2×10^6, 2.34×10^5 and 1.21×10^2 molecules·cm^{-3} at 5, 10 and 15 km altitudes, respectively.

Table S10 Coordinates stationary points for the $HO_2 + SO_3$ reaction without and with *X* (*X* = H_2O, $(H_2O)_2$, H_2SO_4, $H_2SO_4\cdots H_2O$ and $(H_2SO_4)_2$) at the M06-2X/6-311+G(2*df*,2*pd*) level of theory

HO_2

O	0.05495900	0.70692200	0.00000000
O	0.05495900	-0.59859000	0.00000000
H	-0.87934600	-0.86666200	0.00000000

SO_3

S	0.00000000	0.00000000	0.00004200
O	0.00000000	1.22894800	-0.70957800
O	0.00000000	-1.22894800	-0.70957800
O	0.00000000	0.00000000	1.41907300

IM

S	-0.65103500	0.09510600	-0.00000300
O	-1.12311500	-0.41905700	1.23336900
O	-1.12315800	-0.41921800	-1.23329100
O	0.00168700	1.38229700	-0.00009700
O	2.13179700	0.02563700	0.00000200
H	1.62474200	0.89379400	-0.00004500
O	1.21176700	-0.87159600	0.00003000

TS

S	-0.56835000	0.00037700	0.06110100
O	-1.13555000	-1.24032700	-0.31712500
O	-1.13538100	1.23659100	-0.33185300
O	0.16647700	0.00813500	1.35484800
O	2.01351200	-0.00009100	-0.04412500
H	1.31450400	0.00606100	0.93812100
O	1.06333000	-0.00582000	-0.90121400

$HOSO_4$

S	0.45817600	-0.03289000	0.08694800
O	0.30730800	1.14735200	-0.92649700
H	-0.22081500	1.85697100	-0.53058500
O	0.42856000	0.45974200	1.41365000
O	1.40805100	-0.94165100	-0.41900500
O	-2.01578900	-0.01185900	0.00414500
O	-1.01688000	-0.81992500	-0.17986600

$H_2O\cdots HO_2$

O	1.06875500	0.66141400	0.01171800
O	0.97910600	-0.63876500	0.00812200
H	0.00981000	-0.81577500	-0.00322300
O	-1.61563500	-0.02251500	-0.08822100
H	-2.29743800	-0.01648500	0.58559700
H	-1.17018200	0.83118700	-0.03532600

IM_WM1

S	0.84128700	-0.27789400	0.00003400
O	0.27117000	-0.76843600	-1.21913900
O	0.27136100	-0.76822600	1.21935000
O	2.15628900	0.24655900	-0.00016300
H	-1.85551700	-1.27871600	-0.76258100
O	-2.27583700	-0.85682300	-0.00020000
H	-1.85793200	-1.27845000	0.76360600
H	-1.71652500	0.45822900	-0.00001400
O	-1.35554200	1.46470300	-0.00000800
O	-0.07126800	1.50037700	-0.00003700

TS_WM1

S	0.78614400	-0.24277500	0.02292800
O	2.14203000	0.13895600	-0.11285700
O	0.01771000	1.45151600	-0.08795400
O	-1.26219800	1.46036700	0.00451100
O	0.26120700	-0.64710200	1.29556000
O	0.13418400	-0.87229400	-1.11362500
H	-1.43929500	-1.13997000	-0.61478400
O	-2.19846000	-0.78781300	-0.06024600
H	-1.80870600	0.27444700	0.03480400
H	-2.08608300	-1.19912500	0.81002200

IMF_WM1

S	0.70762400	-0.29202900	0.07272100
O	2.06630600	-0.51595600	-0.23279600
O	0.56536600	1.40799600	-0.10103400
O	-0.66345900	1.79447300	0.00416100
O	0.11893800	-0.59163700	1.33280000
O	-0.19801700	-0.75394700	-1.07129400
H	-1.17567100	-0.74675600	-0.75352700
O	-2.52983000	-0.56791900	-0.09738200
H	-2.46339300	0.34331600	0.21494700
H	-2.55735600	-1.10817800	0.69939800

$HO_2\cdots(H_2O)_2$

H	0.96147100	2.13177900	0.63004000
O	0.69884900	1.54744000	-0.08606200
H	1.28314500	0.76015200	-0.04311900
O	1.62710600	-0.98756500	0.07946800
H	0.67954700	-1.21924300	0.06195200
H	2.05172900	-1.51245200	-0.60385200
O	-1.22190200	-0.97042700	0.04321700
O	-1.62729500	0.28482600	-0.03710900
H	-0.78995100	0.84556600	-0.04113500

IM_WD1

H	-3.00639900	1.43058400	-0.04638800
O	-2.26708100	0.99072600	0.38472500
H	-2.36411200	0.01607300	0.20550100
O	-2.39950600	-1.56507300	-0.30322400
H	-1.48892100	-1.64268600	-0.63691900
H	-2.49279900	-2.23560800	0.37971400
O	-0.17953800	2.15482400	-0.27571300
H	-0.99995600	1.53911900	0.04937500
O	0.92813000	1.49505500	-0.46284500
S	1.04201500	-0.49497600	0.11159500
O	0.30852500	-1.07493500	-0.99527800

TS_WD1

H	-2.95846900	1.36812500	-0.12597400
O	-2.25225900	0.93424900	0.36583500
H	-2.30565000	-0.06564900	0.17809400
O	-2.29574600	-1.54691000	-0.28606500
H	-1.38094900	-1.60097300	-0.63099000
H	-2.35456400	-2.19377200	0.42380400
O	-0.21673600	2.07201600	-0.27045400
H	-1.15589000	1.41019300	0.08669200
O	0.91284100	1.45737100	-0.45595700
S	1.02594300	-0.43762300	0.10508800
O	0.32238600	-1.05374100	-1.01007200

O	0.34936300	-0.38021100	1.36590900
O	2.47010000	-0.51887000	0.06932700

O	0.29290600	-0.35633000	1.34324800
O	2.45416200	-0.49614800	0.11183500

IMF_WD1

H	-2.97400100	1.57263500	0.60601700
O	-2.72452300	0.69442700	0.90787600
H	-2.46852500	-0.50261200	-0.25498400
O	-2.10214700	-1.20102900	-0.85703600
H	-0.67323700	-1.20733200	-0.74367900
H	-2.53432000	-2.03093000	-0.63479100
O	0.08313000	1.65186700	-1.14737700
H	-1.81496600	0.76998800	1.23712400
O	1.22524100	1.16881200	-0.73762100
S	1.00929700	-0.23944800	0.29475300
O	0.38371900	-1.23141000	-0.69072600
O	0.07244300	0.16593500	1.30966300
O	2.35167300	-0.59492400	0.59950400

***c*-$HO_2 \cdots H_2SO_4$**

S	0.86352900	-0.05995800	-0.11832700
O	-0.08301400	-1.13466900	0.09686400
O	0.09131500	1.27394300	0.03787000
O	1.68049500	-0.04915700	-1.26888200
O	1.84003100	-0.02503700	1.11109800
H	-0.90156600	1.09729300	0.04687500
H	1.35788200	-0.17442100	1.93504400
O	-2.64478700	-0.60725900	-0.02748700
H	-1.73331000	-1.01138800	-0.02578800
O	-2.45147400	0.67315900	0.04267400

***c*-IM_SA**

S	1.80737200	-0.51138300	0.00060700
O	0.99691000	-0.61240900	1.18438400
O	3.16063400	-0.90880800	0.04465200
O	1.08679400	-0.58665900	-1.24480000
O	1.06947500	2.09552600	-0.00707200
H	0.13170600	1.54254000	-0.05261600
O	2.11447300	1.35780000	0.03186000
S	-2.02253800	0.00463000	-0.01800300
O	-1.71700800	-0.67505200	1.34241800
O	-3.41437500	0.17672500	-0.12452900
O	-1.17481000	1.18941100	-0.12947000
O	-1.54321900	-1.00913500	-1.08399400
H	-0.74691900	-0.74053500	1.47989900
H	-0.57311500	-0.91314100	-1.25651700

***c*-TS_SA1**

S	-1.80491600	-0.48149200	0.00180900
O	-3.15560300	-0.88749100	0.04342100
O	-0.98857200	-0.60726400	1.18315100
O	-1.07684200	-0.58621700	-1.24268100
O	-1.02126600	2.05951200	-0.00359000
H	-0.00582500	1.49025000	-0.05736800
O	-2.08243400	1.34644400	0.02763000
S	2.00664100	-0.01424500	-0.01906100
O	1.48615700	-1.01229000	-1.06783800
O	3.39978800	0.13097400	-0.13210900
O	1.20661800	1.21580600	-0.14758000
O	1.67872400	-0.65053600	1.35092900
H	0.50364700	-0.90391000	-1.22553100
H	0.70202300	-0.72605700	1.46827800

***c*-IMF_SA1**

S	-1.88461100	-0.39379400	-0.06357400
O	-3.17887800	-0.93045200	-0.18791400
O	-1.29789100	-0.62414400	1.31756300
O	-0.87620200	-0.54185000	-1.06998400
O	-1.09358400	1.98081600	-0.00125600
H	0.66920700	1.41080400	-0.49069400
O	-2.18323500	1.29155000	-0.00462100
S	2.07510800	-0.06567200	0.09050200
O	1.83296100	-1.16851900	-0.98233500
O	3.45909700	-0.00258400	0.33451900
O	1.62469800	1.24858500	-0.61594500
O	1.17164800	-0.29524300	1.20439000
H	0.88448600	-1.22341600	-1.20433600
H	-0.27055300	-0.50119800	1.30884100

***t*-$HO_2 \cdots H_2SO_4$**

S	-0.87225200	-0.07063300	-0.11654600
O	0.06468000	-1.14580700	-0.30637300
O	-1.23478000	-0.13395700	1.41776000
O	-2.06980600	-0.00092100	-0.87004800
O	-0.11377400	1.26925900	-0.25306100
H	-2.06234800	0.33982400	1.57606600
H	0.87071300	1.11957400	-0.09540900
O	2.61864700	-0.59087800	-0.01361900
H	1.71770800	-0.99478200	-0.14704200
O	2.41377800	0.68549400	0.09173100

t-IM_SA1

S	-1.85438500	-0.55024600	0.03784300
O	-1.12156200	-0.68421500	-1.20222500
O	-3.21691500	-0.92518800	0.05174600
O	-1.06537600	-0.53904800	1.22279800
O	-1.13762200	2.12011300	0.01354900
H	-0.26014700	1.56180500	0.06127300
O	-2.18038200	1.38108500	-0.08111600
S	2.04783200	0.03119900	-0.05891000
O	1.95670900	-0.60690900	1.37262800
O	1.44454600	-1.03371700	-0.99137500
O	1.15964300	1.16786000	-0.00621100
O	3.40744400	0.22292400	-0.40198400
H	2.74227200	-1.14635600	1.53841500
H	0.45082400	-0.93393200	-1.08508100

t-TS_SA1

S	1.84564300	-0.47141800	-0.04303900
O	1.12965200	-0.64618400	1.22547300
O	3.19822200	-0.87852800	-0.06742300
O	0.99905500	-0.56051500	-1.18810100
O	1.02720300	2.02289500	-0.02163500
H	-0.06080600	1.42628100	-0.07994100
O	2.10554100	1.33881800	0.04318900
S	-1.99982700	-0.01242400	0.07020600
O	-1.93019100	-0.66786200	-1.34821700
O	-1.28249600	-0.95283500	1.00046100
O	-1.21697700	1.22621300	-0.09002900
O	-3.34870300	0.16582500	0.45137600
H	-2.70097100	-1.23671300	-1.48553700
H	-0.22173900	-0.83069500	1.09006500

t-IMF_SA1

S	-1.88641100	-0.41523400	0.07964800
O	-1.22053400	-0.65080700	-1.26518200
O	-3.20690300	-0.90321300	0.09858300
O	-0.95669700	-0.55531800	1.14865400
O	-1.09721600	1.98877500	0.01926800
H	0.37734400	1.30876700	0.20987600
O	-2.17290500	1.29315300	-0.03599800
S	2.04605200	-0.05279500	-0.10265900
O	1.95969100	-0.77547200	1.29257000
O	1.23931200	-0.80428400	-1.05158800
O	1.37441300	1.27835500	0.23832500
O	3.39979900	0.17255000	-0.44778100
H	2.70291100	-1.44014800	1.36722900
H	-0.18620200	-0.73007100	-1.18374100

c-$HO_2\cdots H_2SO_4\cdots H_2O$

O	-2.48491800	-1.43855800	-0.01619600
H	-1.51436400	-1.31289800	-0.18059200
O	-2.98980400	-0.24352000	0.01048900
S	1.15682400	-0.18805500	0.09533300
O	2.32702200	-0.22800700	-0.95662900
O	1.00524700	1.31434900	0.37022500
O	-0.04573500	-0.63535800	-0.57850900
O	1.62833100	-0.88728100	1.23023600
H	2.03415100	0.14344700	-1.79925300
H	0.02834100	1.62464000	0.19878800
O	-1.35883700	1.96917300	-0.07801100
H	-1.91445300	1.16090500	-0.11227400
H	-1.79331300	2.58640700	0.51517400

c-IM_SW1

S	2.09585100	-0.40893100	-0.38124200
O	0.71201500	-0.76900300	-0.53593700
O	3.05265400	-1.42644300	-0.15619500
O	2.49922500	0.81204500	-1.01260400
O	0.85866200	0.46263000	1.94015000
H	-0.01098500	0.21288200	1.34593600
O	2.00446200	0.26195000	1.41132500
S	-2.26260300	-0.19860600	0.02443900
O	-1.89386700	0.79325900	-1.09178500
O	-1.88437500	-1.58997100	-0.56672700
O	-1.39356300	0.06872400	1.16615100
O	-3.65428600	-0.20833800	0.25014000
H	-1.05843600	1.33133200	-0.88180300
H	-0.92003100	-1.64298600	-0.69844300
O	0.14917900	2.18363100	-0.49076400
H	1.00609800	1.97302300	-0.89445400
H	0.05055900	3.13846200	-0.47241400

c-TS_SW1

S	-2.08169800	-0.33004800	0.40833400
O	-0.70412500	-0.68126800	0.64331500
O	-3.05976500	-1.35278300	0.39542400
O	-2.45420400	0.99177600	0.82570600
O	-0.84104000	0.13475300	-1.97468400
H	0.11639600	0.00693200	-1.34644600
O	-1.99005700	-0.01145700	-1.43660600
S	2.23537300	-0.20442500	0.00954700
O	1.86634900	0.90024900	0.99993300
O	1.83559300	-1.52287400	0.72712300
O	1.38423500	-0.04795900	-1.17882000
O	3.62374600	-0.25331700	-0.22447700
H	1.04299300	1.45212500	0.72108700
H	0.87154600	-1.53673100	0.88610000
O	-0.09879600	2.26298100	0.25241900
H	-0.00575000	3.21741800	0.20924300
H	-0.97946000	2.05099900	0.60927200

***c*-IMF_SW1**

S	2.05083200	-0.18668600	-0.42419100
O	0.67236200	-0.47370300	-0.74694400
O	3.09817900	-0.81484900	-1.13456100
O	2.24361200	1.24915200	-0.14074200
O	1.17608200	-0.69641800	1.88152100
H	-0.58298100	-0.58096600	1.09779900
O	2.22598000	-0.87041500	1.15591600
S	-2.32052200	-0.13574100	-0.08388600
O	-1.81198000	1.18331500	-0.42038100
O	-1.90771600	-1.11275400	-1.22205500
O	-1.55894000	-0.64956300	1.17154800
O	-3.70135100	-0.29066000	0.14621400
H	-0.62024900	1.90420800	0.03854200
H	-0.95253900	-1.02407100	-1.40886600
O	0.20511200	2.43135900	0.34859200
H	1.15777500	1.89778400	0.11463800
H	0.18231500	3.31817100	-0.02574400

***t*-$HO_2\cdots H_2SO_4\cdots H_2O$**

O	-2.35841800	-1.43097900	0.10205900
H	-1.42070200	-1.28014700	0.39257400
O	-2.84391400	-0.25179600	-0.13719600
S	1.17701000	-0.16074200	0.11443500
O	0.86833400	-0.60983200	-1.37604300
O	1.12726400	1.36837300	0.05140800
O	0.03790500	-0.63826700	0.85430000
O	2.48970200	-0.57396400	0.45523000
H	1.68790400	-0.60968200	-1.88807400
H	0.14312500	1.69230400	0.04752900
O	-1.29126700	2.00981700	0.07033000
H	-1.64543400	2.58965200	-0.60745000
H	-1.83390300	1.19291700	0.06374800

***t*-IM_SW1**

S	-2.08435400	0.23073000	0.29679100
O	-0.98828400	0.05890700	1.19341700
O	-3.42023700	0.12605500	0.75280000
O	-1.82010600	0.99937000	-0.89277100
O	-0.90616100	-1.93301700	-0.99456000
H	-0.14897100	-1.21224300	-0.86058000
O	-2.04202900	-1.54873000	-0.54198300
S	1.98268300	-0.27246400	0.17196700
O	3.37429500	-0.28960900	-0.57323400
O	1.90144800	1.12578500	0.75230000
O	1.02951300	-0.37936900	-0.92390200
O	1.99403400	-1.26205700	1.18780000
H	4.06210100	-0.57821000	0.04146700
H	1.26802900	1.76319600	0.19077700
O	0.39027800	2.57071700	-0.55019100
H	0.74707100	2.90717500	-1.37629900
H	-0.40352200	2.04341000	-0.77289600

***t*-TS_SW1**

S	-2.05785600	0.17667000	0.27278900
O	-0.95794800	0.09134000	1.18077700
O	-3.39371500	0.07734300	0.73048900
O	-1.80457500	0.97200400	-0.91389000
O	-0.82554000	-1.89476200	-0.94663800
H	0.01952700	-1.11374500	-0.85053100
O	-1.97241200	-1.53530900	-0.50792400
S	1.97355200	-0.22393900	0.18632900
O	3.41038600	-0.24056900	-0.46207600
O	1.89068000	1.18119700	0.66050200
O	1.04042100	-0.38252000	-0.95638400
O	1.90238900	-1.23136400	1.18227400
H	3.76887500	-1.13704400	-0.41905400
H	1.09815900	1.82732100	0.10959900
O	0.25952500	2.50739100	-0.48813400
H	0.60291000	2.87821700	-1.30656900
H	-0.53428800	1.94355000	-0.71131200

***t*-IMF_SW1**

S	2.18473000	-0.32088600	-0.29349800
O	1.03199000	-0.34898700	-1.15516200
O	3.32788100	-1.09826900	-0.57304200
O	2.51084600	1.08901700	0.10746300
O	0.57445400	-0.32351200	1.58668200
H	-0.50831100	-0.87535600	-0.90614800
O	1.62283000	-0.96925800	1.17721700
S	-2.34696500	-0.08537000	-0.17600900
O	-2.29015000	-0.41414500	1.36415500
O	-1.70270300	1.19039700	-0.29885000
O	-1.45012700	-1.17403800	-0.81305900
O	-3.67173300	-0.28036200	-0.64028100
H	-2.92652200	-1.11133100	1.57295300
H	-0.26325500	1.99521700	0.06823700
O	0.56304000	2.52344100	0.14626700
H	1.62543200	1.75193100	0.11662700
H	0.53779000	3.18536300	-0.55065600

$HO_2\cdots(H_2SO_4)_2$

O	0.03126700	2.61618200	0.54548600
H	0.74230500	2.04042100	0.91997500
O	-0.20630600	2.13819900	-0.63613900
S	2.08790100	-0.38737900	0.07232200
O	1.44562500	-1.74738200	-0.28014000
O	1.97744100	0.44678800	-1.24186400
O	1.23205100	0.28370400	1.04983400
O	3.44688700	-0.59239300	0.37758100
H	0.50562400	-1.60691300	-0.56708200
H	1.12100100	0.92171000	-1.26081300
S	-2.01508300	-0.53162200	-0.02230600
O	-2.71131100	0.79521700	-0.46174700
O	-3.03273900	-1.49391400	0.13430900
O	-0.90374900	-0.77080800	-0.92290100
O	-1.40963700	-0.18371000	1.37059300
H	-2.05920900	1.48162000	-0.68731200
H	-0.43103800	-0.06788500	1.31488400

IM_SD1

S	-2.27613700	-1.07355100	-0.48583600
O	-2.74031700	0.28519300	-0.44802300
O	-3.19573000	-2.10544800	-0.76836300
O	-0.88342500	-1.25049400	-0.77529500
O	-1.38261400	-0.59438500	2.06476500
H	-0.84024700	0.07754600	1.43922900
O	-2.19003000	-1.35794600	1.42691600
S	-0.01274300	2.13703500	-0.01204000
O	0.17119700	1.55301500	-1.41642400
O	-1.48140100	2.59206300	-0.04465000
O	0.11278200	1.00544200	0.93679700
O	0.81676400	3.24204000	0.26872700
H	0.89610700	0.84320900	-1.40890000
H	-2.06900700	1.83251300	-0.27664900
S	2.59225900	-0.94690300	-0.13247300
O	1.49742300	-1.96360100	0.32205900
O	3.82055900	-1.61302500	-0.30816300
O	2.03354700	-0.17715800	-1.22445100
O	2.74355000	-0.02658600	1.11775500
H	0.65823100	-1.80750200	-0.15666400
H	1.92241000	0.47606000	1.27536200

TS_SD1

S	-1.73923000	-1.56256100	-0.45273800
O	-2.55426300	-0.44528500	-0.85977800
O	-2.19311500	-2.86970100	-0.73218300
O	-0.32683200	-1.29245300	-0.39438500
O	-1.70358600	-0.49489700	1.99934500
H	-1.06715900	0.27844900	1.39231600
O	-2.11942000	-1.52975600	1.37164400
S	-0.63630000	2.15865600	-0.07727000
O	-0.04028600	1.58964400	-1.35725100
O	-2.14263300	2.05861000	-0.33340000
O	-0.30081300	1.18786200	1.01583200
O	-0.27224700	3.48826300	0.20470000
H	0.84806700	1.09744700	-1.20603500
H	-2.38851800	1.13126000	-0.62269600
S	2.78415800	-0.45562400	-0.02703900
O	2.31742500	-1.89988300	-0.35249900
O	4.18723300	-0.47884000	0.08437900
O	2.16050900	0.46251100	-0.96050900
O	2.15911400	-0.17541200	1.37895900
H	1.34595900	-1.93099300	-0.46797700
H	1.35491500	0.37101500	1.29829400

IMF_SD1

S	-2.29571100	-1.13970700	-0.37430100
O	-2.96228700	0.17936800	-0.69434800
O	-3.03687100	-2.23598300	-0.84998600
O	-0.87278900	-1.03817300	-0.51593900
O	-1.73153800	-0.44747600	1.97377900
H	-0.25226000	0.47763800	1.24093700
O	-2.53607400	-1.21948500	1.32636200
S	-0.11543800	2.15880400	-0.07092700
O	0.26691200	1.52035700	-1.40896800
O	-1.56344500	2.11241200	0.01307500
O	0.44037800	1.12933200	1.00092200
O	0.53566900	3.38891800	0.15534200
H	1.04452600	0.87425100	-1.34401100
H	-2.37082500	1.00458300	-0.45348700
S	2.72061900	-0.94344200	-0.11236800
O	1.55595600	-1.78489600	0.50412600
O	3.83993900	-1.76143700	-0.35921200
O	2.16075100	-0.15897200	-1.19198000
O	3.09661700	0.00148800	1.07069700
H	0.72080800	-1.65420100	0.01280900
H	2.36046900	0.60363200	1.27432400

Reference

[1] J. Gonzalez, M. Torrent-Sucarrat and J. M. Anglada, *Phys. Chem. Chem. Phys.*, 2010, **12**, 2116-2125.

[2] J. M. Anglada, G. J. Hoffman, L. V. Slipchenko, M. M. Costa, M. F. Ruiz-Lopez and J. S. Francisco, *J. Phys. Chem. A*, 2013, **117**, 10381-10396.

[3] J. Liu, S. Fang, Z. Wang, W. Yi, F. M. Tao and J. Y. Liu, *Environ. Sci. Technol.*, 2015, **49**, 13112-13120.

[4] L. Liu, J. Zhong, H. Vehkamäki, T. Kurtén, L. Du, X. H. Zhang, J. S. Francisco and X. C. Zeng *Proc. Natl. Acad. Sci. U. S. A.*, 2019, **116**, 24966-24971.

[5] X. T. Le, T. V. T. Mai, K. C. Lin and L. K. Huynh, *J. Phys. Chem. A*, 2018, **122**, 8259-8273.

[6] X. T. Le, T. V. T. Mai, M. V. Duong and L. K. Huynh, *Chem. Phys. Lett.*, 2019, **728**, 142-147.

[7] T. V. T. Mai, M. V. Duong, H. T. Nguyen and L. K. Huynh, *Phys. Chem. Chem. Phys.*, 2018, **20**, 6677-6687.

[8] T. V. T. Mai, P. Raghunath, X. T. Le, L. K. Huynh, P. C. Nam and M. C. Lin, *Chem. Phys. Lett.*, 2014, **592**, 175-181.

[9] T. V. T. Mai, A. Ratkiewicz, M. V. Duong and L. K. Huynh, *Chem. Phys. Lett.*, 2016, **646**, 102-109.

[10] T. V. T. Mai, M. V. Duong, H. T. Nguyen, K. C. Lin and L. K. Huynh, *J. Phys. Chem. A*, 2017, **121**, 3028-3036.

[11] T. V. T. Mai, M. V. Duong, H. T. Nguyen, K. C. Lin and L. K. Huynh, *Chem. Phys. Lett.*, 2018, **706**, 280-284.

[12] T. V. T. Mai and L. K. Huynh, *Phys. Chem. Chem. Phys*., 2019, **21**, 17232-17239.

[13] T. V. T. Mai, H. T. Nguyen and L. K. Huynh, *Phys. Chem. Chem. Phys*., 2019, **21**, 23733-23741.

[14] T. V. T. Mai, H. T. Nguyen and L. K. Huynh, *Atmos. Environ.*, 2020, **242**, 117833.

[15] T. Zhang, K. Zhai, Y. Zhang, L. Geng, Z. Geng, M. Zhou, Y. S. Lu, X. Z. Shao and M. Lily, *Comput. Theor. Chem*., 2020, **1176**, 112747.

[16] M. A. Ali, M. Balaganesh and S. Jang, *Atmos. Environ.*, 2019, **207**, 82-92.

[17] S. Ghoshal and M. K. Hazra, *RSC Adv.*, 2015, **5**, 17623-17635.